Expanding Naloxone Accessibility: A Lifesaver or a Risky Setback?

Junyang Cai, Noa Zychlinski
Faculty of Data and Decision Science, Technion – Israel Institute of Technology, Haifa, 3200003, Israel,
junyang.cai@campus.technion.ac.il, noazy@technion.ac.il

The widespread prevalence of opioids has prompted governments to implement targeted interventions aimed at reducing overdose mortality, with naloxone accessibility emerging as one of the most prominent policies. Naloxone, a potent opioid antagonist, is highly effective in reversing overdoses, yet its expanded availability introduces complex trade-offs, particularly in the presence of moral hazard.

We develop a dynamic compartmental model that captures transitions between susceptible individuals and those with opioid use disorder (OUD), allowing us to evaluate the impact of naloxone accessibility on overdose mortality and to derive the optimal accessibility policy. We show that full naloxone accessibility is optimal in the absence of moral hazard or when its effect is small. However, when moral hazard is significant—where greater access to naloxone encourages riskier opioid use—expanded accessibility can paradoxically increase overdose deaths.

Extending the model to incorporate peer-driven contagion in opioid misuse, we find that the structure of the optimal policy remains robust, preserving the bang-bang nature and the reversal induced by moral hazard. Two additional insights emerge under this interaction-based model. First, in epidemics primarily driven by prescription-induced opioid use, full accessibility remains optimal. In contrast, when opioid use spreads socially—especially as the effectiveness of naloxone declines due to potent synthetic opioids like carfentanil—limited accessibility may become preferable. Second, the relationship between naloxone accessibility and overdose mortality may become non-monotonic, exhibiting an inverted U-shape in which moderate increases in accessibility can initially worsen outcomes.

A calibrated case study based on U.S. data suggests that under current epidemic conditions, full accessibility remains optimal—a finding that aligns with existing regulatory policies. However, our results highlight that shifts in epidemic dynamics, such as increased opioid potency or heightened social contagion, may fundamentally alter this conclusion. These findings underscore the need for continuous reevaluation of naloxone distribution policies as the opioid crisis evolves.

Key words: opioid epidemic, naloxone accessibility, moral hazard, mathematical model, healthcare management

1. Introduction

The opioid epidemic is a growing global crisis, with the U.S. experiencing particularly severe impacts. Opioids – including heroin, tramadol, and fentanyl – are widely prescribed for pain relief but are highly susceptible to misuse, leading to dependency and addiction. For individuals who

overdose, the risk of respiratory depression is significant, and without the timely administration of the opioid antagonist naloxone, the likelihood of suffocation and death rises dramatically.

A 2019 investigation from World Health Organization reported that approximately 600,000 people worldwide died from drug-related causes, with nearly 80% of those deaths attributed to opioids. Moreover, the opioid epidemic in the U.S. worsened during the COVID-19 pandemic, as many individuals turned to illicit synthetic fentanyl to cope with mental health issues such as anxiety and depression (Haley and Saitz 2020, Abramson 2021). According to the National Institute on Drug Abuse, the annual number of deaths related to opioid overdoses in the U.S. was approximately 50,000 between 2017 and 2019, surged to 68,630 in 2020 and further increased to 81,806 in 2022.

The staggering number of deaths caused by opioid abuse poses a grave threat to public health and well-being, making it imperative for governments to implement policies aimed at reducing opioid-related mortality. One direct solution is to enhance the accessibility of naloxone, enabling individuals to promptly administer this life-saving medication in the event of an overdose. Specifically, classifying naloxone as a non-prescription medicine and allowing individuals with opioid use disorder (OUD) to take it home has helped increase access to this medication (Hardin et al. 2024).

Several countries have adopted such measures in recent years. In 2023, the U.S. Food and Drug Administration (FDA) approved Narcan, a nasal spray form of naloxone, for over-the-counter (OTC) use, allowing individuals to purchase this vital medication without a prescription. Canada and Australia implemented similar policies in 2016 and 2022, respectively, and Sweden is now preparing to follow suit to reduce overdose deaths (Euractiv 2024).

While many view these policies as critical, life-saving interventions for individuals struggling with addiction (Ardeljan et al. 2023, Qayyum et al. 2023), others raise concerns about unintended consequences. Expanding naloxone access may inadvertently encourage riskier opioid use by giving individuals an exaggerated sense of protection. For instance, Sally Satel, a psychiatrist and drug policy scholar, noted, *"Patients occasionally tell me that having naloxone on hand has served as insurance against overdose. So, in some instances, it enhances risk taking"* (The Washington Post, 2018).

This ongoing debate underscores the need for analytical tools that can quantify the trade-offs between increased accessibility and potential behavioral risks. While expanding naloxone accessibility can undoubtedly improve survival rates during overdose events, many experts agree that it is unlikely to serve as a standalone solution to the opioid crisis. Critics argue that increased access may inadvertently encourage riskier drug use or fail to address the root causes of addiction. For example, The Washington Free Beacon published an opinion piece in 2024, saying expanding naloxone accessibility is unlikely to significantly mitigate the opioid epidemic or serve as a long-term solution (The Washington Free Beacon 2024). Critics have voiced concerns regarding the

White House's endorsement of OTC naloxone. Recently, harm reduction vending machines providing naloxone were removed in response to public concerns in British Columbia, although naloxone has been approved as OTC medicine for many years in Canada (The Tyee 2024). Opposition to expanding naloxone access has also been voiced in policy discussions, with arguments suggesting it does not address the underlying causes of the opioid crisis (Maine Beacon 2022). Furthermore, expanding naloxone accessibility may result in unintended consequences, including a potential increase in overdose risk among individuals with OUD, as naloxone can induce withdrawal effects (Kline et al. 2020).

The benefits of enhancing accessibility to naloxone are already evident in certain areas. For instance, in Connecticut, the government's widespread distribution of naloxone effectively halted the rise in opioid-related deaths in 2022 and 2023 (CT Insider 2024). Similarly, Massachusetts and New Jersey have also demonstrated this positive trend (Boston.com 2024, New Jersey Monitor 2024). However, it is important to note that while the number of opioid-related deaths in Connecticut has decreased, the number of individuals with OUD remains high, or possibly even higher than before. Furthermore, not all regions have achieved their intended targets of reducing deaths. According to Cambrian News, deaths involving opioids are becoming more frequent, even though the number of individuals with OUD carrying naloxone has continuously increased in Wales (Cambrian News 2024).

Another notable example is Colorado, where The Naloxone Project has aimed to expand access to this life-saving medication since 2021. Despite these efforts, the state has not seen a corresponding decline in fatalities (The Colorado Sun 2024). Similarly, a study of opioid overdose deaths in Hamilton County, Ohio, and neighboring regions found that increased naloxone access did not consistently translate into reduced mortality (Freiermuth et al. 2023).

Figure 1 further illustrates this pattern by presenting opioid overdose deaths in Canada from 2016 to 2023. Although the Canadian government approved naloxone as an OTC medication in 2016 (Government of Canada 2024), overdose deaths have continued to rise, suggesting that expanded access alone may be insufficient to curb the epidemic.

These varying outcomes across regions raise two central questions: (1) How does expanding naloxone accessibility affect overdose mortality? (2) What level of accessibility minimizes opioid-related deaths?

To address these questions, we develop and analyze mathematical models that capture the complex dynamics of the opioid epidemic, explicitly incorporating the relationship between naloxone accessibility, overdose mortality, and the emergence of new individuals with opioid use disorder (OUD), while accounting for both moral hazard and peer-driven contagion in opioid misuse. Our framework enables us to evaluate how naloxone accessibility influences overdose outcomes and

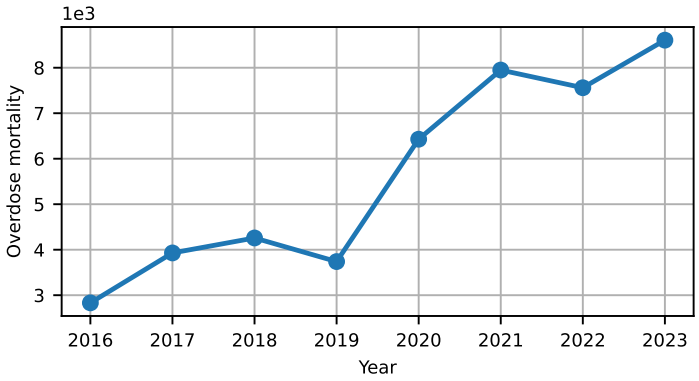

Figure 1 **The number of opioid overdose deaths in Canada from 2016 to 2023 (Data source: Government of Canada).**

to derive structured policies that balance life-saving benefits against potential unintended consequences. Despite the urgency and societal relevance of this issue, it remains largely underexplored in the operations research (OR) and operations management (OM) literature.

1.1. Contributions

The paper makes the following key contributions:

- ***An operational modeling framework for naloxone accessibility.*** We introduce a mathematical framework to analyze the opioid crisis, combining a Susceptible-Addicted-Susceptible (SAS) structure with explicit modeling of naloxone accessibility. This framework captures both the dynamic interplay between opioid use and overdose mortality, and the policy levers available to public health authorities. To our knowledge, this is the first analytical model to operationalize naloxone access decisions within an epidemic-inspired structure, enabling transparent evaluation of trade-offs between overdose prevention and behavioral risks.
- ***Structured characterization of optimal accessibility under moral hazard.*** We derive a sharp policy structure for optimal naloxone accessibility by formulating and solving an optimization problem that minimizes overdose mortality while explicitly accounting for moral hazard—where greater accessibility may encourage riskier opioid consumption. The presence of moral hazard yields non-trivial policy reversals: full accessibility, though intuitively appealing, may cease to be optimal when the behavioral response to naloxone undermines its benefits.

While policymakers are generally aware of the trade-off between naloxone's life-saving potential and its unintended consequences, our model formalizes this tension and provides an explicit threshold that delineates when expanded access is socially optimal. This threshold offers a practical tool: it connects empirical estimates of behavioral response to policy design, allowing decision-makers to continuously evaluate whether expanded access remains justified or more restrictive policies are warranted.

- ***Robustness of optimal policy under social contagion dynamics.*** Our results reveal that the structure of the optimal policy remains robust even when incorporating peer-driven contagion in opioid misuse. In particular, the switching behavior induced by moral hazard persists under social contagion dynamics, but new complexities emerge. Specifically, while full naloxone accessibility is optimal when prescription misuse dominates, limited accessibility may become preferable in socially driven epidemics—especially as more potent synthetic opioids, such as carfentanil, reduce naloxone's effectiveness.

A calibrated case study based on U.S. data demonstrates the framework's practical relevance. It suggests that, under current epidemic conditions, full accessibility remains optimal—a finding that aligns with existing regulatory policies. However, this outcome is contingent on present-day dynamics. Our model shows that future shifts, such as increased opioid potency may fundamentally alter optimal policies.

Additionally, we identify a non-monotonic relationship between accessibility and overdose mortality: while greater access can reduce mortality in some settings, it may initially worsen outcomes in others, following an inverted U-shaped pattern. Together, these insights highlight the importance of continuous, evidence-based reevaluation of naloxone policies as the opioid crisis evolves, ensuring that interventions remain both effective and responsive to changing conditions.

1.2. Organization

The remainder of the paper is structured as follows. Section 2 reviews the related literature. From Section 3 to Section 6, we sequentially develop four models to characterize the progression of the opioid epidemic and conduct corresponding analyses. We begin with a basic SAS model with opioid prescription-induced addiction in Section 3, and then progressively incorporate two key elements in the subsequent sections: (1) the potential moral hazard arising from naloxone and (2) the transmission dynamics of opioid addiction driven by the social interactions between the susceptible and OUD populations. See Table 1 for an overview of the structure and focus of these four sections. Next, to illustrate and validate our modeling framework, Section 7 provides a case

Table 1 Paper organization: Sections 3 to 6.

	No moral hazard	Moral hazard present
Prescription-induced	SAS (Section 3)	SAS-M (Section 4)
Social + Prescription-induced	D-SAS (Section 5)	D-SAS-M (Section 6)

study based on data from the U.S. Finally, Section 8 concludes the paper and outlines directions for future research. All technical proofs are provided in the electronic companion.

2. Literature review

The widespread impact and equity concerns of the opioid crisis in the U.S. significantly fueled research across various disciplines. We began by reviewing the related OR/OM literature, followed by a brief overview of relevant fields, including public health, economics, and medicine.

Zaric et al. (2000) were among the first to address opioid addiction management in OR/OM. They analyzed the U.S. drug crisis, highlighting the cost-effectiveness of expanding methadone use to treat heroin addiction and reduce HIV transmission. Using a dynamic compartmental model, they found that increased access to methadone maintenance improved the quality of life for individuals with OUD. Although research on the opioid crisis waned in subsequent years, it recently regained significant attention.

Since an opioid overdose can cause suffocation within a short golden window, the use of drones to rapidly deliver life-saving medication became crucial for those overdosing without naloxone on hand. Research by Gao et al. (2024) and Lejeune and Ma (2025) focused on naloxone distribution using drones. Both studies established optimization models to reduce response time and decrease mortality rates. Ansari et al. (2024) combined a dynamic compartmental model with a Markov decision process to generate optimal budget allocations for better-formulated intervention policies aimed at combating the opioid epidemic. Similarly, Luo and Stellato (2024) integrated a dynamic model with a mixed-integer programming problem to address opioid treatment facility locations and treatment budget allocations. Their method effectively increased treatment opportunities for individuals with OUD. Recently, Baucum et al. (2025) developed a predict-then-optimize framework to reallocate substance use treatment centers across U.S. counties, balancing overdose mortality reduction with equity and equality in access. In the context of the opioid epidemic, Gökçınar et al. (2022) developed a pain management framework for prescription opioids to balance pain relief and opioid addiction. Recently, Gan et al. (2025) proposed a constrained partially observable MDP to model the health states as well as transitions of patients with OUD, aiming to optimize personalized treatment strategies delivered through wearable devices.

In addition to these studies, several papers employed empirical approaches to investigate the opioid crisis. Studies by Yang and Mishra (2025), Liu and Bharadwaj (2020), Bobroske et al. (2022), KC et al. (2022), and Attari et al. (2024) aimed to reveal relationships between the opioid epidemic and factors such as the internet, drug supply chain, and race, offering insights for effective management and response strategies.

Beyond the opioid epidemic, several studies used epidemiological models to examine operational questions related to the COVID-19 pandemic.

Li et al. (2023) developed an effective epidemiological tool to predict COVID-19 cases, deaths, and the effects of government interventions. The model informed the selection of vaccine trial sites

by forecasting COVID-19 incidence under different intervention scenarios. A data-driven approach to optimize COVID-19 vaccine distribution was later proposed by Bertsimas et al. (2022), integrating the epidemiological model with a prescriptive optimization model for vaccination site locations and allocation. The method demonstrated the potential to increase vaccination effectiveness while ensuring fairness across states and robustness to uncertainties.

Chen and Kong (2023) presented an epidemiological model that integrated the effects of limited medical resources to assess their influence on COVID-19 transmission and mortality. The study examined three hospital admission policies, comparing their effects on infection, mortality, and bed occupancy, particularly under constrained medical capacity. The findings emphasized the importance of timely interventions and indicated that a one-time lockdown policy could be as effective as a bed-triggered policy if implemented at the appropriate stage of the outbreak.

Although several OR/OM studies addressed opioid prevalence and mitigation, systematic research on the link between naloxone accessibility and the opioid epidemic remained limited. To address this gap, this paper developed and analyzed stylized mathematical models to provide insights into the managerial and policy implications of naloxone accessibility, tackling a critical issue of public health and societal importance.

We concluded this section with a brief review of relevant studies in economics, public health, and medicine. In these fields, naloxone accessibility remained a topic of significant debate. A substantial body of research in public health and medicine supported expanding naloxone accessibility. For example, Rao et al. (2021) employed a dynamic compartmental model to project that overdose-related deaths could reach 1,220,000 by 2029 in the U.S. Their analysis indicated that a 30% increase in naloxone accessibility could avert 25% of these deaths. Jawa et al. (2022) strongly advocated for increased naloxone access and OTC availability, suggesting that insurance companies should reimburse individuals with OUD for naloxone. Similar recommendations are provided in Burris et al. (2009), Houser (2023), Messinger et al. (2023), Saberi et al. (2024).

In contrast, several economic studies raise concerns about behavioral side effects of naloxone accessibility, often framed as moral hazard (e.g., Doleac and Mukherjee 2022, Packham 2022). Our study also examines this mechanism, which reflects individuals' tendency to engage in riskier behavior when protected from the full consequences. The concept of moral hazard originated in traffic safety research, where safer vehicles were shown to encourage reckless driving, offsetting some safety gains through higher pedestrian fatalities and non-fatal accidents (Peltzman 1975). Similar unintended consequences have been documented in finance and insurance. For example, government guarantees can lead banks to anticipate future bailouts, prompting banks to adopt riskier investment strategies and resulting in moral hazard (Pernell and Jung 2024).

In the context of the opioid crisis, Doleac and Mukherjee (2022) and Packham (2022) argued that expanding naloxone access may have mixed effects, as it could unintentionally encourage riskier drug use. Similarly, Spencer (2023) and Liu et al. (2025) showed that decriminalization policies, which increased drug accessibility, were followed by unexpected rises in overdose deaths. Our findings also relate to Cawley and Dragone (2024), who examined how introducing less harmful substitutes – such as methadone for opioid use – can improve health outcomes, but under certain conditions may also lead to unintended consequences.

Building on this literature, our analysis provides a structured, operational model that explicitly captures how naloxone accessibility, moral hazard, and evolving epidemic dynamics jointly influence overdose mortality. We formally characterize the conditions under which increased accessibility can either save lives or unintentionally worsen public health outcomes.

3. The Basic SAS Model

Our basic SAS model, which is illustrated in Figure 2, comprises two groups: $S(t)$, representing the number of susceptible individuals at time t, and $A(t)$, denoting the number of individuals with OUD at time t.

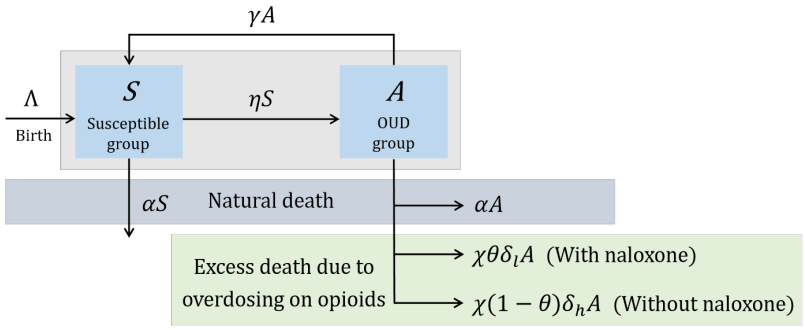

Figure 2 **The illustration of the basic SAS model.**

We denote by $\Lambda > 0$ the inflow rate into the susceptible group, capturing births and potential immigration, and by $\alpha > 0$ the outflow rate from both groups, representing natural deaths and possible emigration. Similar to Luo and Stellato (2024), in our basic model, we assume that new individuals with OUD are generated at a transition rate $\eta > 0$ from the susceptible group. This transition pattern can be interpreted as patients spontaneously developing OUD as a result of opioid prescription induction.

In the case of an overdose, $\delta_l \in (0,1)$ and $\delta_h \in (0,1)$ denote the mortality rates at the individual level, with δ_l being lower when timely treatment with naloxone is provided, and δ_h being higher when such treatment is unavailable. That is, $\delta_h > \delta_l$. The rate at which overdose events occur

among individuals with OUD is denoted as $\chi > 0$. The decision variable is $\theta \in [0,1]$, representing the accessibility of naloxone within the OUD group (i.e., the proportion of individuals with OUD who possess naloxone). Note that $\theta = 1$ indicates that all individuals with OUD have access to naloxone during an overdose emergency, while $\theta = 0$ indicates that no individuals with OUD have access to naloxone during an overdose emergency. It is important to emphasize that in our model, θ reflects naloxone accessibility through *public channels*. Zero accessibility does not imply that naloxone is entirely unavailable; rather, it indicates that public distribution would not be optimal under certain conditions. Naloxone may still be strictly prescribed or administered in special clinical settings by healthcare professionals as medically appropriate. Similar regulatory structures exist in practice; for example, in the U.S., methamphetamine (commonly referred to as *Ice*) is classified as a Schedule II controlled substance (Drug Enforcement Administration 2024). While its general use is strictly prohibited, limited medical administration remains permitted under strict supervision in exceptional clinical situations.

While our model primarily focuses on naloxone accessibility for individuals with OUD, we acknowledge that expanding naloxone access extends beyond this group to the general public. By increasing community-wide availability, policymakers aim to ensure that bystanders can intervene during an overdose, reinforcing the broader public health objective of reducing opioid-related mortality across society.

Lastly, we denote by $\gamma > 0$ the rate at which individuals with OUD successfully overcome their active use through medication-assisted treatment or other therapeutic methods. Recognizing the potential for relapse, we also account for individuals who, after successful detoxification, may revert to active use.

In the basic model, we assume that opioid overdose rates are uniform across the OUD population, regardless of naloxone possession. In other words, possessing naloxone does not lead to increased opioid consumption or overdose. This assumption aligns with a widely accepted perspective within parts of the public health community (New York Times 2024, Tse et al. 2022). In Section 4, we incorporate a moral hazard, which suggests an increased risk of opioid overdose among individuals with OUD who possess naloxone, as argued by some economic studies (Doleac and Mukherjee 2022, Packham 2022).

Furthermore, in Section 5 and Section 6, we introduce two model extensions in which the generation of new individuals with OUD could be influenced by interactions between the susceptible and OUD groups – an approach aligns with the framework of infectious model prevalent in epidemiology, which has been proposed in several studies as a suitable representation of the opioid overuse crisis (Ansari et al. 2024, Cole et al. 2024).

The dynamics of the basic SAS model are described by the following system of differential equations:

$$\begin{cases} \dot{S}(t) = \Lambda - (\alpha+\eta)\, S(t) + \gamma A(t), \\ \dot{A}(t) = \eta S(t) - (\alpha+\gamma+\chi\theta\delta_l + \chi(1-\theta)\delta_h)\, A(t), \\ S(t), A(t) \geq 0. \end{cases} \tag{1}$$

Note that the overall mortality rate regarding overdose in model (1) is $(\chi\theta\delta_l + \chi(1-\theta)\delta_h)$.

3.1. Optimization and Analysis

We begin by deriving the equilibrium point, (S^*, A^*), for the basic model described in (1):

$$(S^*, A^*) = \left(\frac{\Lambda\left(\chi(\theta\delta_l + (1-\theta)\delta_h) + \alpha + \gamma\right)}{\alpha(\alpha+\gamma+\eta) + \chi(\alpha+\eta)(\theta\delta_l + (1-\theta)\delta_h)}, \frac{\eta\Lambda}{\alpha(\alpha+\gamma+\eta) + \chi(\alpha+\eta)(\theta\delta_l + (1-\theta)\delta_h)} \right).$$

Recognizing that fatal outcomes from opioid abuse represent the primary concern for both policymakers and society (CNN 2017, Reider 2019), our objective is to minimize the long-run average opioid overdose mortality. Specifically, we seek to solve:

$$\begin{aligned} \min_{\theta\in[0,1]} \quad \mathcal{D}(\theta) &:= \lim_{T\to\infty} \frac{1}{T} \int_0^T \chi(\theta\delta_l + (1-\theta)\delta_h) A(t)\, \mathrm{d}t \\ &= \chi(\theta\delta_l + (1-\theta)\delta_h) A^* \\ &= \frac{\eta\Lambda\chi(\theta\delta_l + (1-\theta)\delta_h)}{\alpha(\alpha+\gamma+\eta) + \chi(\alpha+\eta)(\theta\delta_l + (1-\theta)\delta_h)}. \end{aligned} \tag{2}$$

PROPOSITION 1 **(Optimal accessibility for the SAS model)**. *For problem (2), full naloxone accessibility is optimal.*

Proposition 1 establishes that full naloxone accessibility minimizes opioid overdose mortality. Intuitively, broader naloxone availability increases the likelihood of survival during overdose events among individuals with OUD. This result aligns with widely held views that advocate for universal access to naloxone (e.g., The Washington Post, 2023). Furthermore, it is consistent with current FDA regulations, which support its approval as an OTC medication and emphasize the importance of maximizing its accessibility.

4. Accounting for Moral Hazard in SAS-M Model

The *moral hazard* phenomenon, also known as the *Peltzman effect* (Peltzman 1975), has been widely discussed in relation to the opioid crisis. Moral hazard is an economic concept describing the tendency of individuals to take riskier actions when they can mitigate or avoid the consequences of those risks. A classic and illustrative example of moral hazard pertains to traffic safety: for instance, Sagberg et al. (1997) observed that taxi drivers operating vehicles equipped with Anti-lock Braking Systems (ABS) tend to wear seatbelts less frequently compared to those driving taxis without ABS.

In the context of the opioid crisis, there is growing concern that easier access to naloxone may encourage riskier opioid consumption behavior among individuals with OUD, leading to higher misuse rates. Specifically, individuals may consume opioids in a compensatory manner, assuming naloxone will mitigate the risk of fatal overdose. Some economic studies have used econometric methods to provide evidence of moral hazard in this context (Doleac and Mukherjee 2022, Packham 2022). Furthermore, individuals who overdose and are revived with naloxone often experience severe withdrawal symptoms, which can increase the likelihood of immediate opioid reuse (Greene 2018).

However, some public health experts challenge these findings, arguing that moral hazard is either negligible or irrelevant in the context of the opioid crisis (New York Times 2024, Tse et al. 2022). They emphasize that the life-saving benefits of naloxone far outweigh the speculative risks of increased opioid misuse.

Although the existence and extent of moral hazard remain a subject of debate, we believe it is crucial to consider its potential impact on the opioid crisis and the optimal design of naloxone accessibility policies. Ignoring moral hazard risks may result in incomplete or suboptimal strategies for addressing opioid misuse and overdose fatalities. To this end, we introduce $\Delta > 0$ to represent the degree of moral hazard among individuals with OUD who have access to naloxone, reflecting the increase in overdose risk due to behavioral changes stemming from naloxone availability. A larger Δ reflects a greater likelihood of opioid overuse within this group.

The SAS-M model incorporating moral hazard is in the following system of differential equations:

$$\begin{cases} \dot{S}(t) = \Lambda - (\alpha+\eta)\, S(t) + \gamma A(t), \\ \dot{A}(t) = \eta S(t) - (\alpha+\gamma+(\chi+\Delta)\delta_l\theta + \chi\delta_h(1-\theta))\, A(t), \\ S(t), A(t) \geq 0, \end{cases}$$

where $(\chi+\Delta)\delta_l\theta + \chi\delta_h(1-\theta)$ is the overall mortality rate regarding opioid overdose and $(\chi+\Delta)\delta_l\theta$ represents the mortality rate of the OUD group possessing naloxone at a moral hazard level Δ. Clearly, there are additional $\Delta\delta_l\theta A(t)$ deaths involving opioids at time t.

4.1. Optimization and Analysis

We begin by deriving the equilibrium point (S_M^*, A_M^*) for the SAS-M model:

$$(S_M^*, A_M^*) = \left(\frac{\Lambda\left(\alpha+\gamma+\chi(\theta\delta_l+(1-\theta)\delta_h)+\Delta\delta_l\theta\right)}{\alpha(\alpha+\gamma+\eta)+(\alpha+\eta)(\chi(\theta\delta_l+(1-\theta)\delta_h)+\Delta\delta_l\theta)}, \frac{\eta\Lambda}{\alpha(\alpha+\gamma+\eta)+(\alpha+\eta)(\chi(\theta\delta_l+(1-\theta)\delta_h)+\Delta\delta_l\theta)} \right).$$

The corresponding optimization objective for the SAS-M model is given by

$$\begin{aligned} \min_{\theta\in[0,1]} \mathcal{D}_M(\theta) &:= \lim_{T\to\infty} \frac{1}{T}\int_0^T \left(\chi(\theta\delta_l+(1-\theta)\delta_h)+\Delta\delta_l\theta\right) A(t)\,\mathrm{d}t \\ &= \left(\chi(\theta\delta_l+(1-\theta)\delta_h)+\Delta\delta_l\theta\right) A_M^* \\ &= \frac{\eta\Lambda\left(\chi(\theta\delta_l+(1-\theta)\delta_h)+\Delta\delta_l\theta\right)}{\alpha(\alpha+\gamma+\eta)+(\alpha+\eta)(\chi(\theta\delta_l+(1-\theta)\delta_h)+\Delta\delta_l\theta)}. \end{aligned} \tag{3}$$

As evident from (3), both the direct life-saving benefits of naloxone and the adverse effects of moral hazard contribute to overdose mortality through the term $\chi((1-\theta)\delta_h + \theta\delta_l) + \Delta\delta_l\theta$. In particular, for any fixed level of accessibility θ, we have $\partial\mathcal{D}_M/\partial\Delta > 0$, indicating that an increase in moral hazard directly increases overdose mortality and may, therefore, contradict the public health objective of reducing overdose deaths.

To formally capture the tension between opposing forces from moral hazard and naloxone accessibility, we next define the neutral effect threshold associated with moral hazard:

$$\bar{\Delta} := \frac{\chi(\delta_h - \delta_l)}{\delta_l} > 0.$$

In other words, $\bar{\Delta}$ represents the critical threshold at which naloxone accessibility yields a neutral effect on overdose mortality. Specifically, when $\Delta = \bar{\Delta}$, the total overdose mortality rate, $(\chi + \bar{\Delta})\delta_l\theta + \chi\delta_h(1-\theta)$, simplifies to $\chi\delta_h$, which is independent of the accessibility level θ.

Theorem 1 characterizes the optimal naloxone accessibility policy in the presence of moral hazard.

THEOREM 1 **(Optimal accessibility for the SAS-M model)**. *For problem (3), full accessibility is optimal if $\Delta < \bar{\Delta}$, and no accessibility is optimal otherwise.*

For clarity and consistency throughout the paper, the boundary case $\Delta = \bar{\Delta}$ is combined with the case where no accessibility is optimal. We note, however, that at this threshold, any accessibility yields identical overdose mortality levels and is therefore optimal. More generally, we classify any non-unique optimal policy that includes zero accessibility as a zero-accessibility policy by default throughout the paper.

According to Theorem 1, when moral hazard is relatively mild, the life-saving benefits of naloxone outweigh its adverse behavioral effects, making full accessibility optimal. Conversely, when moral hazard becomes sufficiently large, the negative consequences dominate, and restricting accessibility becomes preferable. Limiting access in this case helps mitigate overdose risk and prevents further loss of life. This bang-bang structure, in which the optimal policy lies at one of the extremes, is common in healthcare management models (Mehrez and Gafni 1987, Chehrazi et al. 2019).

Figure 3 illustrates the effect of naloxone accessibility on overdose mortality across varying levels of moral hazard. When moral hazard is relatively low ($\Delta < \bar{\Delta} = 0.06$), increasing naloxone accessibility leads to a decline in overdose mortality, highlighting the life-saving benefits of broader naloxone availability in settings with limited risk compensation behavior. In contrast, when moral hazard is high ($\Delta > \bar{\Delta}$), greater naloxone accessibility results in *higher* overdose mortality, suggesting that excessive reliance on naloxone may encourage riskier opioid use behaviors that outweigh its protective effect. At the threshold level ($\Delta = \bar{\Delta}$), overdose mortality is independent of naloxone accessibility, indicating a tipping point at which the positive and negative effects of accessibility are

balanced. Furthermore, holding naloxone accessibility θ constant, an increase in moral hazard consistently leads to higher overdose mortality, reinforcing the detrimental role of risk compensation in undermining public health interventions.

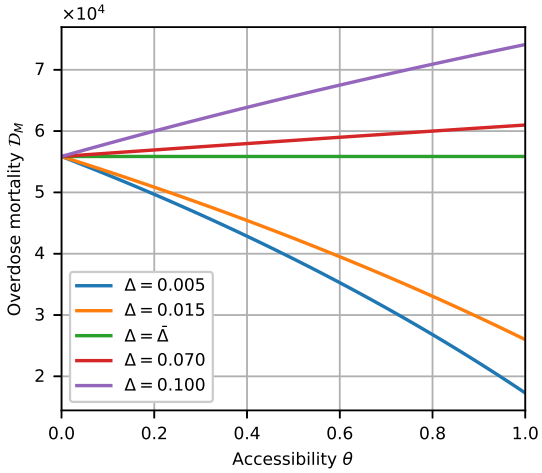

Figure 3 **Naloxone accessibility effect on overdose mortality $\mathcal{D}_M$. The parameters are:** $\Lambda = 2 \times 10^5$, $\alpha = 0.01$, $\eta = 0.09$, $\chi = 0.012$, $\delta_h = 0.75$, $\delta_l = 0.125$, $\gamma = 0.1$, $\bar{\Delta} = 0.06$.

5. The D-SAS Model Incorporating Social Interaction

In this section, we extend our analysis by developing a more comprehensive model inspired by epidemiological frameworks commonly used to study the opioid crisis (e.g., Battista et al. 2019, Cole and Wirkus 2022, Cole et al. 2024). These studies demonstrate that opioid misuse can be effectively represented using epidemiological approaches, as its spread often follows patterns similar to infectious disease transmission, driven by social interactions and peer influence. The emergence of new cases of OUD depends on contacts between individuals at risk and those already affected, leading to nonlinear growth dynamics analogous to disease outbreaks.

Similar to infectious diseases, where contact between infected and susceptible individuals accelerates transmission, opioid use frequently expands through social networks and environmental exposure. Individuals with OUD may influence others directly or indirectly, contributing to the initiation of opioid use through interpersonal relationships and community-level factors. Empirical evidence supports this dynamic, showing that opioid misuse often emerges from peer networks, community settings, or family environments (Luthar et al. 1992, Worsham and Barnett 2020, Rockett et al. 2024, Adamopoulou et al. 2024).

We introduce the D-SAS model, which incorporates two pathways for the initiation of OUD: a constant-rate term, as in the original SAS model, and an interaction term that accounts for new

cases arising from interactions between susceptible individuals and those already diagnosed with OUD. In Section 6, we further extend the model to include the effects of moral hazard. A similar combined framework was previously applied by Ansari et al. (2024) in the context of the opioid crisis.

We adopt the *standard incidence* form, $\beta\frac{S(t)A(t)}{N(t)}$, to model the interaction between susceptible individuals and individuals with OUD, where β denotes the transmission rate, and $N(t) = S(t) + A(t)$ represents the total population at time t. This formulation is commonly used in epidemiological models of the opioid crisis (e.g., Cole and Wirkus (2022), Cole et al. (2024)). The underlying assumption is that opioid transmission primarily occurs within localized and bounded social networks, where individuals tend to interact repeatedly within specific peer groups and communities (Mars et al. 2014). As a result, the likelihood of interaction depends on the proportion of individuals in each group rather than their absolute numbers (Martcheva 2015).

The D-SAS model is governed by the following system of differential equations:

$$\begin{cases} \dot{S}(t) = \Lambda - (\alpha+\eta)\, S(t) - \beta\dfrac{S(t)A(t)}{N(t)} + \gamma A(t), \\ \dot{A}(t) = \eta S(t) + \beta\dfrac{S(t)A(t)}{N(t)} - (\alpha+\gamma+\chi\theta\delta_l + \chi(1-\theta)\delta_h)\, A(t), \\ S(t), A(t) \geq 0. \end{cases} \tag{4}$$

Remark 1. To ensure the robustness of our results, we also analyze an alternative formulation based on the *mass action incidence* form, $\beta S(t)A(t)$, which has been used in previous studies of opioid use dynamics (e.g., Djilali et al. 2017, Huang and Liu 2013). The optimal accessibility policy for the D-SAS model under mass action incidence is provided in Appendix EC.1. While the solution formulations are slightly different, the overall structure of the solution and the key insights remain consistent, demonstrating the robustness of the results.

5.1. Optimization and Analysis

We denote the equilibrium of the D-SAS model by (S_D^*, A_D^*), where closed-form expressions are provided in Appendix EC.2. The corresponding optimization problem aims to minimize the long-run average overdose mortality, given by:

$$\begin{aligned} \min_{\theta\in[0,1]} \quad \mathcal{D}_D(\theta) &:= \lim_{T\to\infty}\frac{1}{T}\int_0^T (\chi\theta\delta_l + \chi(1-\theta)\delta_h)\, A(t)\,\mathrm{d}t \\ &= \chi(\theta\delta_l + (1-\theta)\delta_h)A_D^*. \end{aligned} \tag{5}$$

Before characterizing the optimal naloxone accessibility policy for the D-SAS model in Theorem 2, we introduce the following auxiliary terms:

$$\omega_l := (\alpha-\beta+\gamma+\eta)^2 + 4\beta\eta + 2\chi\delta_l(\alpha-\beta+\gamma+\eta),$$

$$\omega_h := (\alpha-\beta+\gamma+\eta)^2 + 4\beta\eta + 2\chi\delta_h(\alpha-\beta+\gamma+\eta).$$

Note that when $\beta > \alpha+\gamma+\eta$, it holds that $\omega_l > \omega_h$.

THEOREM 2 **(Optimal accessibility for the D-SAS model)**. *For problem (5), the optimal naloxone accessibility policy is as follows:*

1. ***Full accessibility is optimal*** *if any of the following conditions holds:*

a. $\beta \leq \alpha+\eta+\gamma$;

b. $\beta > \alpha+\eta+\gamma$ *and* $\omega_h \geq 0$;

c. $\beta > \alpha+\eta+\gamma$, $\omega_h < 0$, $\omega_l > 0$, *and* $\mathcal{D}_D(\theta=1) < \mathcal{D}_D(\theta=0)$.

2. ***No accessibility is optimal*** *if any of the following conditions holds:*

a. $\beta > \alpha+\eta+\gamma$ *and* $\omega_l \leq 0$;

b. $\beta > \alpha+\eta+\gamma$, $\omega_h < 0$, $\omega_l > 0$, *and* $\mathcal{D}_D(\theta=0) \leq \mathcal{D}_D(\theta=1)$.

According to Theorem 2, the optimal accessibility level in the D-SAS model remains either full or zero. Full accessibility is optimal when the primary driver of the opioid crisis is the spontaneous onset of opioid use following medical prescriptions (Case 1a, i.e., when η is relatively large). This result is consistent with the findings from the basic SAS model (Proposition 1).

However, when opioid use is primarily driven by peer influence and social transmission (i.e., for large enough values of β such that $\beta > \alpha+\eta+\gamma$), full accessibility may no longer be optimal (Cases 2a and 2b).

At least for now, naloxone is still highly effective in reversing opioid overdoses, with a success rate ranging from 75% to 100% (Rzasa and Galinkin 2018), implying that δ_l is typically small and thus $\omega_l \leq 0$ is less likely. Nevertheless, the growing prevalence of carfentanil – an opioid estimated to be 100 times more potent than fentanyl – raises concerns (New York Post 2024). Naloxone may be less effective in reversing overdoses caused by such high-potency substances, which would increase δ_l and make Cases 2a and 2b more relevant. This concern is further supported by recent evidence suggesting that high-dose naloxone is not necessarily more effective in such scenarios (STAT 2024). As a result, if carfentanil or similar ultra-potent opioids become more widespread in the future, the assumptions underlying the current optimal policy may no longer hold, and policies regarding naloxone distribution and usage would need to be carefully reexamined.

In addition, according to Theorem 2, we observe a counterintuitive outcome: when the overdose rate χ becomes sufficiently high, restricting naloxone accessibility may be socially optimal. Under the condition of $\beta > \eta+\alpha+\gamma$, both thresholds ω_h and ω_l decline with increasing overdose rate χ, maybe causing the system to transition from Cases 1b to Cases 2a in the parameter space. Intuitively, this reflects a scenario where expanding naloxone access reduces overdose mortality in the short term but reinforces social dynamics that fuel OUD prevalence. When baseline overdose rates are already high, this unintended consequence can offset the benefits of naloxone, ultimately leading to more deaths. This analysis provides policymakers with a quantitative framework to

identify such tipping points, highlighting when increased accessibility could backfire under specific epidemic conditions.

Next, Figure 4 illustrates the optimal naloxone accessibility policy θ^* under the D-SAS model across a range of OUD onset rates η and transmission rates β. The figure partitions the (η, β) space into five distinct regions, each corresponding to a different case in Theorem 2. The region enclosed by the solid black line comprises two areas (Cases 2a and 2b), where zero accessibility is optimal. In contrast, the area outside the black line includes three regions (Cases 1a, 1b, and 1c), where full accessibility is optimal. In other words, holding other parameters fixed, full accessibility

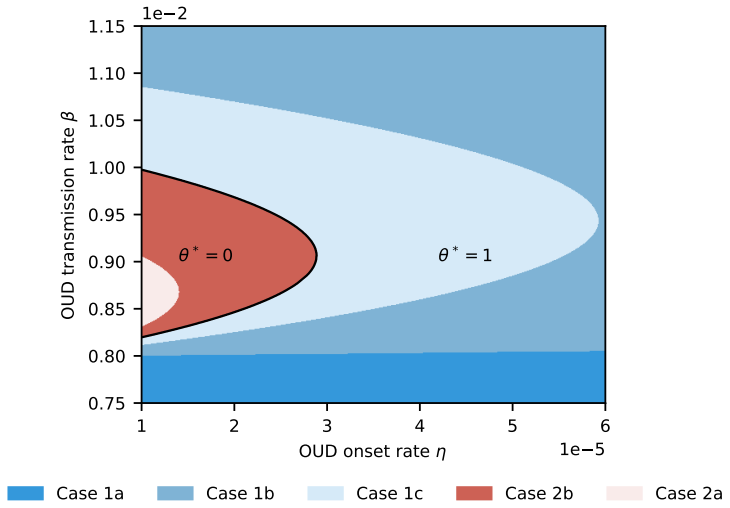

Figure 4 **The optimal policy structure for the D-SAS model regarding β and η on the basis of D-SAS model. The parameters are $\Lambda = 2 \times 10^5$, $\gamma = 0.002$, $\alpha = 0.006$, $\delta_h = 0.75$, $\delta_l = 0.35$, $\chi = 0.002$.**

is optimal when either β is relatively small or large, or when η is relatively large. When β is small, peer influence plays a limited role in opioid initiation, so increasing naloxone accessibility reduces mortality without triggering broader behavioral responses. When β is large, social transmission may nonlinearly pull more susceptibles into the OUD group, enlarging the population exposed to overdose risk; hence, broadening naloxone accessibility is crucial to offset the corresponding rise in preventable deaths.

As for η, a high spontaneous initiation rate means that many individuals begin opioid use independently of social exposure. In such scenarios, the societal benefits of wide naloxone availability outweigh the risks, justifying full accessibility. Conversely, when β is moderate and η is low, opioid use remains relatively contained. In these cases, increasing accessibility has limited impact on reducing deaths, making zero accessibility the optimal policy.

Lastly, note that while overdose mortality under Cases 1a, 1b, and 2a exhibits a monotonic relationship with accessibility – either consistently decreasing or increasing – this is not the case in Cases 1c and 2b. This is because, in these two cases, mortality follows an inverted U-shaped pattern, where modest increases in accessibility may initially raise mortality before eventually reducing it at higher levels. This non-monotonic behavior, illustrated in Figure 5, highlights that marginal increases in naloxone accessibility can, in fact, be detrimental. Accordingly, in such cases, identifying the optimal level of accessibility requires comparing the outcomes at the two extreme values, $\theta = 0$ and $\theta = 1$. This non-monotonicity has important policy implications. Empirical findings by

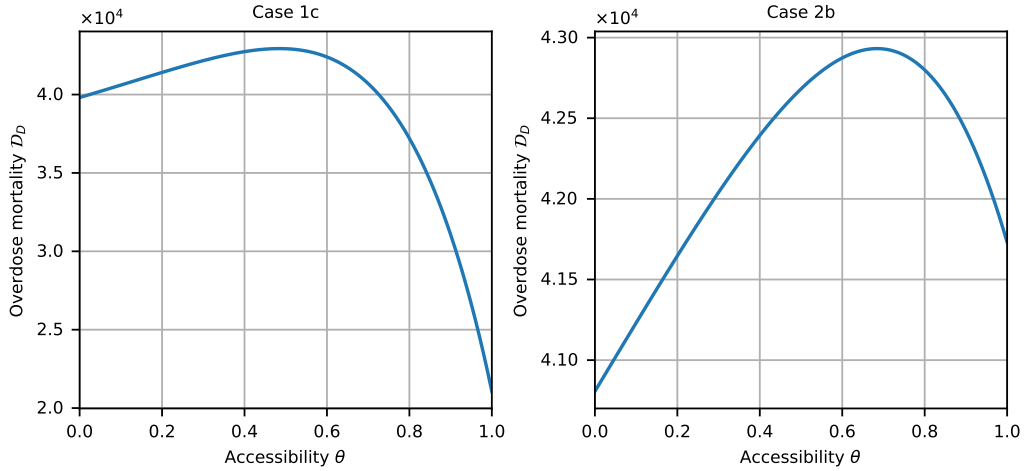

Figure 5 **The impact of naloxone accessibility θ on overdose mortality. The specific parameter values used for each plot are provided in Table EC.2 in Appendix EC.5.**

Packham (2022) show that modest expansions in syringe service programs promoting naloxone access may increase opioid-related deaths, although this trend is not observed for more substantial expansions (Lambdin et al. 2023). While this result – often referred to as a *measurement problem* – has faced criticism in public health circles (New York Times 2024), our model suggests that such a counter-intuitive phenomenon is theoretically plausible. Modest increases in naloxone accessibility may fail to offset the increase in opioid misuse they trigger due to wider social interactions, potentially resulting in higher overdose mortality.

6. Accounting for Moral Hazard in D-SAS-M Model

We now incorporate moral hazard into the D-SAS model, resulting in the D-SAS-M model, whose dynamics are governed by the following system of differential equations:

$$\begin{cases} \dot{S}(t) = \Lambda - (\alpha+\eta)\, S(t) - \beta \dfrac{S(t)A(t)}{N(t)} + \gamma A(t), \\ \dot{A}(t) = \eta S(t) + \beta \dfrac{S(t)A(t)}{N(t)} - (\alpha+\gamma+(\chi+\Delta)\theta\delta_l + \chi(1-\theta)\delta_h)\, A(t), \\ S(t), A(t) \geq 0, \end{cases}$$

where $N(t) = S(t) + A(t)$.

6.1. Optimization and Analysis

We denote the equilibrium of the D-SAS-M model by $(S^*_{D,M}, A^*_{D,M})$. Due to the complexity of the expressions, their closed-form representations are provided in Appendix EC.2.

The corresponding optimization problem that minimizes the long-run average overdose mortality is given by:

$$\begin{aligned} \min_{\theta\in[0,1]} \quad \mathcal{D}_{D,M}(\theta) &:= \lim_{T\to\infty} \frac{1}{T} \int_0^T ((\chi+\Delta)\theta\delta_l + \chi(1-\theta)\delta_h)\, A(t)\, \mathrm{d}t \\ &= ((\chi+\Delta)\theta\delta_l + \chi(1-\theta)\delta_h) A^*_{D,M}. \end{aligned} \tag{6}$$

For brevity, before stating Theorem 3, we define the auxiliary term:

$$\omega_{l,M} := (\alpha-\beta+\gamma+\eta)^2 + 4\beta\eta + 2(\chi+\Delta)\delta_l(\alpha-\beta+\gamma+\eta).$$

When $\beta > \alpha+\gamma+\eta$, we have $\omega_l > \omega_{l,M}$. In this case, $\omega_{l,M} > \omega_h$ if and only if $\Delta < \bar{\Delta}$; otherwise, $\omega_{l,M} < \omega_h$.

THEOREM 3 **(Optimal accessibility for the D-SAS-M model)**. *For problem (6), the optimal naloxone accessibility policy is as follows:*

1. ***Full accessibility is optimal*** *if any of the conditions in Table 2 holds.*

Table 2 Conditions under which full accessibility ($\theta = 1$) is optimal

Case	Δ vs. $\bar{\Delta}$	β vs. $\alpha+\eta+\gamma$	ω_h, $\omega_{l,M}$	Additional Condition
a.	$\Delta < \bar{\Delta}$	$\beta \leq \alpha+\eta+\gamma$	–	–
b.	$\Delta < \bar{\Delta}$	$\beta > \alpha+\eta+\gamma$	$\omega_h \geq 0$	–
c.	$\Delta > \bar{\Delta}$	$\beta > \alpha+\eta+\gamma$	$\omega_h \leq 0$	–
d.	$\Delta < \bar{\Delta}$	$\beta > \alpha+\eta+\gamma$	$\omega_h < 0$, $\omega_{l,M} > 0$	$\mathcal{D}_{D,M}(\theta=1) < \mathcal{D}_{D,M}(\theta=0)$
e.	$\Delta > \bar{\Delta}$	$\beta > \alpha+\eta+\gamma$	$\omega_h > 0$, $\omega_{l,M} < 0$	$\mathcal{D}_{D,M}(\theta=1) < \mathcal{D}_{D,M}(\theta=0)$

2. ***No accessibility is optimal*** *if any of the conditions in Table 3 holds.*

Table 3 Conditions under which zero accessibility ($\theta = 0$) is optimal

Case	Δ vs. $\bar{\Delta}$	β vs. $\alpha+\eta+\gamma$	ω_h, $\omega_{l,M}$	Additional Condition
a.	$\Delta \geq \bar{\Delta}$	$\beta \leq \alpha+\eta+\gamma$	–	–
b.	$\Delta \leq \bar{\Delta}$	$\beta > \alpha+\eta+\gamma$	$\omega_{l,M} \leq 0$	–
c.	$\Delta \geq \bar{\Delta}$	$\beta > \alpha+\eta+\gamma$	$\omega_{l,M} \geq 0$	–
d.	$\Delta \leq \bar{\Delta}$	$\beta > \alpha+\eta+\gamma$	$\omega_h < 0$, $\omega_{l,M} > 0$	$\mathcal{D}_{D,M}(\theta=0) \leq \mathcal{D}_{D,M}(\theta=1)$
e.	$\Delta \geq \bar{\Delta}$	$\beta > \alpha+\eta+\gamma$	$\omega_h > 0$, $\omega_{l,M} < 0$	$\mathcal{D}_{D,M}(\theta=0) \leq \mathcal{D}_{D,M}(\theta=1)$

6.2. Numerical Examples and A Comparison to the SAS-M Model

According to Theorem 3, Figure 6 illustrates how the optimal naloxone accessibility policy depends on the overdose mortality rates δ_l and δ_h, representing mortality with and without naloxone, respectively. The blank area in the figure reflects an infeasible region where the condition $\delta_l < \delta_h$ does not hold.

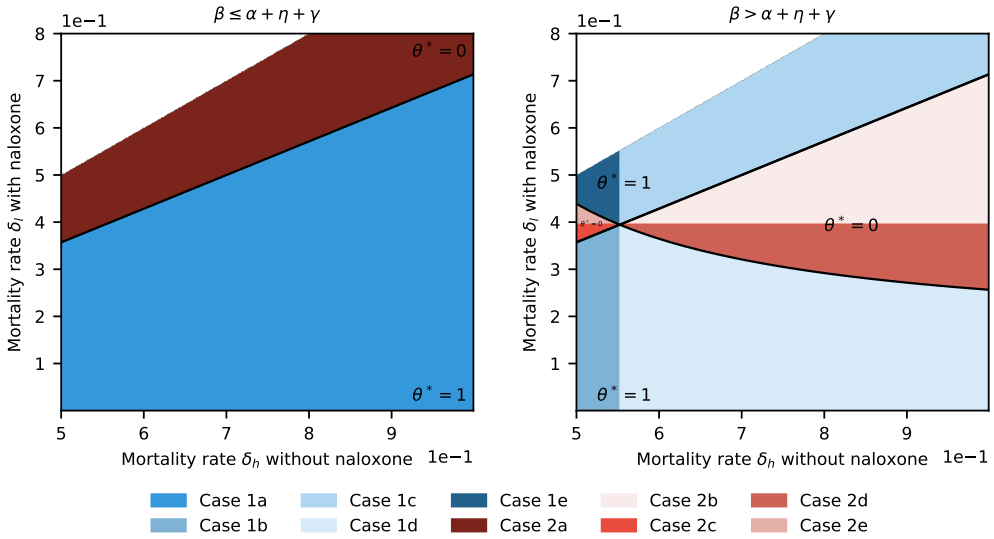

Figure 6 The impact of mortality rate δ_l and δ_h on the optimal accessibility θ^* on the basis of D-SAS-M model. $\Delta = 0.005$ and $\chi = 0.0125$ for both plots. Other specific parameter values used for each plot are provided in Table EC.3 in Appendix EC.5.

The effectiveness of naloxone increases as the difference $(\delta_h - \delta_l)$ grows, with smaller values of δ_l indicating greater life-saving potential. Consequently, when the parameter combination (δ_h, δ_l) lies sufficiently far from the blank region, particularly when δ_l is small, full accessibility is more likely to be optimal in both panels of Figure 6.

The black upward-sloping straight lines in both plots of Figure 6 represent the set of (δ_h, δ_l) pairs for which the neutral effect threshold $\bar{\Delta}$ equals the degree of moral hazard Δ. Parameter

combinations below each line correspond to settings where $\bar{\Delta} > \Delta$, meaning the life-saving benefits of naloxone outweigh its unintended impact on opioid misuse. Conversely, combinations above the curve reflect cases where $\bar{\Delta} < \Delta$, implying that moral hazard dominates the benefits of naloxone.

We begin by examining the left panel of Figure 6, which represents opioid crises primarily driven by prescription opioid addiction (i.e., the SAS-M model or the D-SAS-M model with $\beta \leq \eta + \alpha + \gamma$). In this case, the black curve partitions the parameter space into two distinct regions, corresponding to Cases 1a and 2a from Theorem 3. Below the curve, full accessibility is optimal, whereas above the curve, zero accessibility is optimal. Thus, in this case, the optimal naloxone policy depends solely on the comparison between $\bar{\Delta}$ and Δ.

In contrast, the right panel of Figure 6 represents the D-SAS-M model with $\beta > \eta + \alpha + \gamma$, where social transmission drives the crisis. Here, the optimal policy structure becomes more complex and may reverse above the black curve compared to the left panel. Thus, the black upward-sloping straight line no longer solely determines the policy outcome.

Specifically, Cases 1c and 1e demonstrate that full accessibility may be optimal even when the moral hazard exceeds the neutral threshold ($\Delta > \bar{\Delta}$). As δ_l and δ_h increase, the likelihood that ω_h and $\omega_{l,M}$ become negative also rises, making these cases more prevalent. In other words, when opioid misuse becomes more lethal, strong social diffusion and high moral hazard may still justify expanding naloxone accessibility to reduce overall overdose deaths—despite limited individual-level effectiveness. Note that in these cases, full accessibility leads to a higher overall mortality rate in the D-SAS-M model: $(\chi + \Delta)\delta_l > \chi\delta_h$. This implies that increasing naloxone accessibility may accelerate the rate at which individuals with OUD exit the population, thereby reducing the exposure of susceptible individuals to those with OUD. Over the long term, this dynamic can mitigate the adverse effects of social contagion and ultimately reduce overdose events. This observation is reminiscent of the classical *virulence–transmissibility trade-off* (Kun et al. 2023), which posits that highly lethal viruses are less likely to spread widely. We interpret this result with caution: at the macro level, moral hazard may be less detrimental than traditionally assumed. However, we emphasize that from an individual-level perspective, moral hazard remains a serious concern. While our case study finding in Section 7 suggests that Cases 1c and 1e are less likely to characterize current real-world conditions, the emergence of increasingly potent opioid substances could make these scenarios more relevant in the future. We therefore recommend that policymakers exercise greater caution and prepare proactively for such potential developments.

Conversely, Cases 2b and 2d illustrate that zero accessibility may be optimal despite the immediate life-saving benefits of naloxone. In these cases, the relative advantage of naloxone's effectiveness (δ_l) over the mortality rate without it (δ_h) is marginal. Given the high moral hazard risks associated with these scenarios, the optimal policy may be to restrict accessibility entirely.

Figure 7 illustrates the optimal naloxone policy under the D-SAS-M model as a function of the transmission rate β and the onset rate η. The left plot reflects cases where moral hazard Δ does not exceed the neutral threshold $\bar{\Delta}$, while the right plot shows the opposite. Each plot includes five distinct policy regions. When moral hazard is small (left panel), the optimal policy resembles

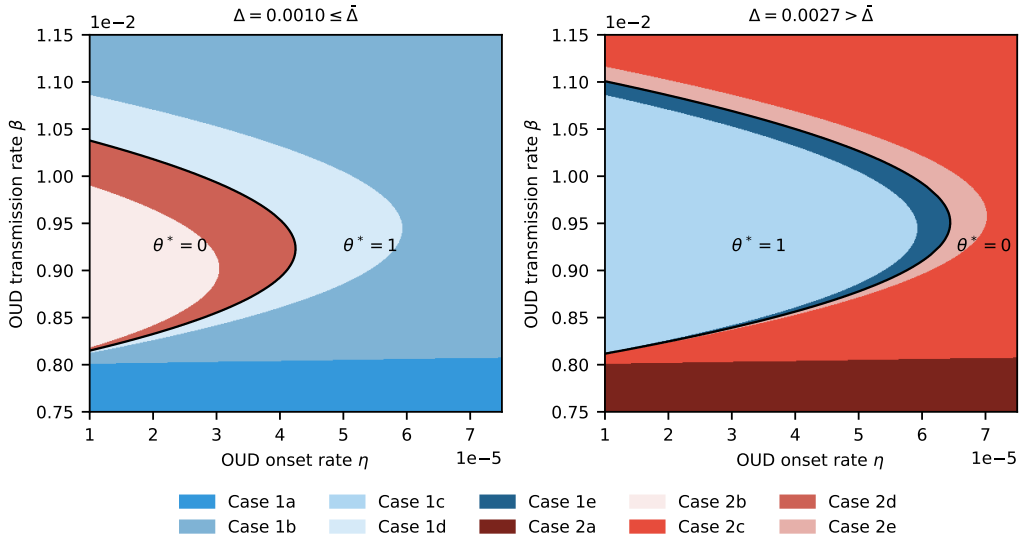

Figure 7 **The optimal policy structure regarding β and η on the basis of D-SAS-M model. The parameters for both plots are $\Lambda = 2 \times 10^5$, $\gamma = 0.002$, $\alpha = 0.006$, $\delta_h = 0.75$, $\delta_l = 0.35$, $\chi = 0.002$, $\bar{\Delta} = 0.0023$.**

the structure of the D-SAS model in Figure 4. However, when moral hazard is substantial (right panel), the policy structure reverses: optimal accessibility is 1 inside the region enclosed by the solid black curve and 0 outside.

As shown in the right plot, when both β and η are high, optimal accessibility drops to zero. In this case, elevated social transmission or onset rates increase overdose risk, and expanding naloxone access amplifies moral hazard, worsening the crisis. Full accessibility remains optimal only when β is moderate and η is low. Under these conditions, both social transmission and prescription-induced opioid use remain contained, and the negative consequences brought by moral hazard do not escalate significantly.

Under Cases d and e in Tables 2 and 3, the D-SAS-M model exhibits a unique inverted U-shaped relationship between accessibility θ and overdose mortality $\mathcal{D}_{D,M}$, as shown in Figure 8. This pattern, preserved by the D-SAS-M model, further supports the empirical findings of Packham (2022) under certain parameter configurations.

Figure 8 also reveals a counterintuitive outcome: stronger moral hazard does not always increase overdose deaths when social contagion is present. Holding accessibility constant at $\theta = 0.4$ (left)

and $\theta = 0.6$ (right), higher moral hazard is associated with lower overdose mortality. Although this result may seem surprising from a policy perspective, the model suggests that in some cases, moral hazard could indirectly reduce long-term mortality by limiting the spread of OUD. An explicit analysis of this phenomenon is provided in Appendix EC.3.

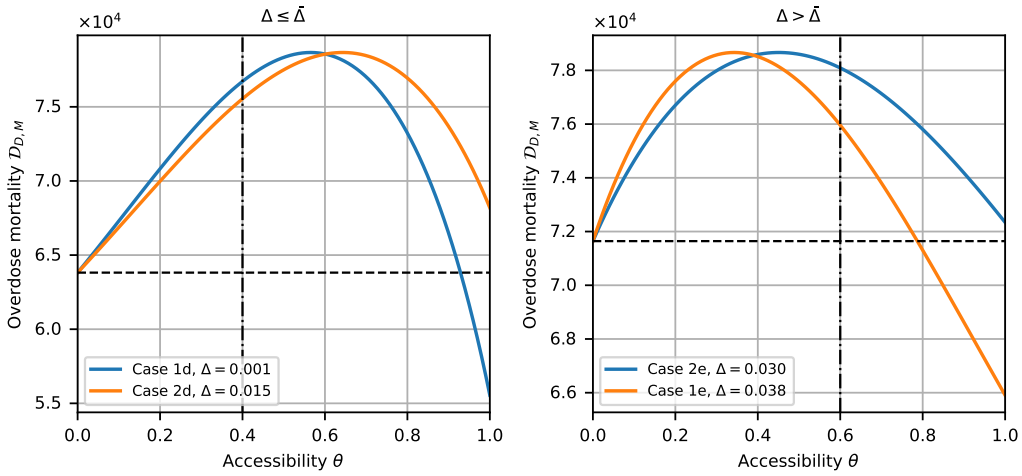

Figure 8 **The impact of naloxone accessibility θ on overdose mortality on the basis of D-SAS-M model. For each plot, except for the moral hazard level, the other parameters remain the same, as detailed in Table EC.4 in Appendix EC.5.**

7. Case Study

To demonstrate the optimal accessibility policy and its real-world applicability, we conduct a case study based on data from the United States. We begin with the calibration of model parameters, followed by the presentation of key findings and a sensitivity analysis. The section concludes with a prospective analysis exploring the potential emergence of next-generation ultra-potent synthetic opioids.

7.1. Calibration of Model Parameters

We begin by calibrating the model based on demographic and opioid-related data from the U.S. To avoid underestimating Λ, we incorporate both the annual number of births and new immigrants, as the U.S. is a major destination for immigration. Notably, annual immigration accounts for approximately one-fourth of total births, making it a significant demographic component. Using data from the Centers for Disease Control and Prevention (CDC) on births and the Office of Homeland Security Statistics on immigration, we calculate the average combined annual inflow (births and new immigrants) for 2010 – 2019. Accordingly, we set $\Lambda = 4{,}977{,}864$.

To estimate the natural death rate α, we use U.S. population data from the U.S. Census Bureau, total mortality data from the CDC, and opioid overdose deaths from CDC WONDER, covering 2010 – 2019. We subtract opioid-related deaths from total deaths to isolate mortality from all other causes and estimate α via regression (see Appendix EC.4), obtaining $\alpha = 0.0083$. It is worth noting that, when estimating α, we do not account for emigration from the U.S. to other countries, as the number of such emigrants is considered negligible. For instance, during the first quarter of 2024, only 344 individuals chose to renounce their U.S. citizenship and emigrate to other countries (Andrew Mitchel International Tax Blog 2024).

We next calibrate the opioid-specific parameters. Based on Rzasa and Galinkin (2018), naloxone successfully reverses 75% – 100% of overdoses. We conservatively set $\delta_l = 1 - (0.75 + 1)/2 = 0.125$. For individuals without access to naloxone, overdose survival depends on emergency medical services (EMS). Ornato et al. (2020) report that the risk of death increases by 10% for every minute of delayed resuscitation. Survey data from Jakubowski et al. (2018) indicate that 43% of respondents had witnessed at least one overdose, and we optimistically assume all witnesses call EMS. Given typical EMS response times of 7 – 8 minutes (Johnson et al. 2021), we approximate the death rate without naloxone as:

$$\delta_h = (1 - 0.43) + 0.43 \times \frac{0.7 + 0.8}{2} = 0.8925.$$

For the recovery rate γ, Luo and Stellato (2024) set the recovery rate at 0.1 for individuals receiving treatment for OUD. However, only approximately 22% of individuals with OUD receive such treatment (National Institute on Drug Abuse, 2023; Jones et al. 2023). Accordingly, we approximate the overall recovery rate as: $\gamma = 0.1 \times 0.22 = 0.022$. For the OUD onset rate η, Battista et al. (2019) assume an annual opioid prescription rate of 0.15 per person and an OUD induction rate of 0.00744 among those prescribed. Thus, $\eta = 0.15 \times 0.00744 = 0.001116$.

To estimate the overdose rate χ, we first approximate the overall opioid-related mortality rate, which is expressed as $\chi(\delta_h(1-\theta) + \delta_l\theta)$ in both the SAS and D-SAS models, and as $\chi(\delta_h(1-\theta) + \delta_l\theta) + \Delta\theta\delta_l$ in the SAS-M and D-SAS-M models. To this end, we use time series data on the U.S. OUD population from 2010 to 2019 provided by Keyes et al. (2022), combined with opioid-related mortality data. Based on these datasets, we construct a regression model to estimate the total opioid-related mortality rate, which is found to be 0.0038 (see Appendix EC.4 for details). That is,

$$\chi(\delta_h(1-\theta) + \delta_l\theta) = 0.0038 \tag{7}$$

in the SAS and D-SAS models or

$$\chi(\delta_h(1-\theta) + \delta_l\theta) + \Delta\theta\delta_l = 0.0038 \tag{8}$$

in the SAS-M and D-SAS-M models.

According to Ornato et al. (2020), fewer than 5% of witnesses administered naloxone to opioid overdose victims in the U.S. prior to 2020. This suggests that the likelihood of immediate naloxone administration, denoted by θ, can be reasonably approximated as 5% during this period. Substituting this value into (7), we obtain:

$$\chi = \frac{0.0038}{0.05 \times 0.125 + 0.8925 \times 0.95} = 0.004449,$$

which applies to both SAS and D-SAS models.

Estimating the moral hazard parameter Δ is particularly challenging (when moral hazard exists), as behavioral responses to naloxone access are not directly observable. However, empirical studies offer useful proxies. Difference-in-differences and other quasi-experimental designs exploit variation in naloxone access laws to assess their effects on opioid misuse, crime, and health outcomes (Rees et al. 2017, Doleac and Mukherjee 2022, Packham 2022). Survey-based studies further document behavioral responses to overdose prevention programs (Wagner et al. 2010, Doe-Simkins et al. 2014). Packham (2022), for instance, report an 18.8% increase in emergency room visits following the implementation of syringe exchange programs that promote naloxone distribution. This increase reflects moral hazard effects. As a simple proxy, we assume that moral hazard contributes to 18.8% of the original overdose rate, implying $\Delta = 0.188\chi$. Substituting this relation into (8) yields:

$$\chi = \frac{0.0038}{0.05 \times 0.125 + 0.8925 \times 0.95 + 0.188 \times 0.05 \times 0.125} = 0.004443 \quad \text{and} \quad \Delta = 0.000835$$

in the SAS-M and D-SAS-M models.

Finally, we estimate the transmission rate β in the D-SAS-M model using a regression-based approach, yielding $\beta = 0.036782$ (see Appendix EC.4 for details). This implies that, on average, each person in the U.S. has approximately 0.036782 effective contacts per year that could result in the transmission of OUD (Hethcote 2000).

The next section presents the case study findings and assesses the robustness of the results through sensitivity analysis.

7.2. Case Study Findings

We now present the representative cases for each model, derived from the calibrated parameter estimates. As summarized in Table 4, full accessibility consistently emerges as the optimal policy across all models, even when accounting for social transmission dynamics. This finding reinforces the FDA's recommendation to expand naloxone access as a central strategy for reducing overdose mortality in the context of the opioid crisis.

Moreover, the observed difference $\bar{\Delta} - \Delta$ suggests that the moral hazard effect remains relatively mild. This indicates that, at present, naloxone's high efficacy in reversing opioid-induced respiratory

Table 4 **Representative cases for each model using calibrated parameters.**

Model	$\bar{\Delta}-\Delta$	$\beta-(\eta+\alpha+\gamma)$	ω_h	ω_l	$\omega_{l,M}$	Corresponding case	θ^*
SAS	–	–	–	–	–	–	1
SAS-M	0.02644502	–	–	–	–	–	1
D-SAS	–	0.005366	0.00015037	0.0001870	–	Case 1b in Theorem 2	1
D-SAS-M	0.02644502	0.005366	0.00015043	–	0.0001859	Case 1b in Theorem 3	1

depression continues to outweigh potential compensatory increases in opioid misuse, supporting its role as an effective harm reduction measure.

In addition, we observe that $\beta-(\eta+\alpha+\gamma)>0$, indicating that social interaction plays a critical role in sustaining the opioid crisis in the U.S. Indeed, despite a steady decline in opioid prescribing rates (American Medical Association, 2021), the crisis remains severe. As emphasized by Dasgupta et al. (2018), although the misuse of prescribed opioids contributes to the development of OUD, the crisis is fundamentally rooted in broader socioeconomic factors and social instability. These findings underscore the importance of incorporating social transmission mechanisms into epidemic models to better capture the persistent, socially driven dynamics of opioid addiction.

Sensitivity Analyses. We also examine how varying levels of moral hazard and overdose rate influence the optimal naloxone accessibility policy in the SAS-M and D-SAS-M models. The estimates of the overdose rate χ and moral hazard Δ are jointly constrained to satisfy $\chi\left(\delta_h(1-\theta)+\delta_l\theta\right)+\Delta\theta\delta_l=0.0038$. As the overdose rate increases, the estimated moral hazard decreases, leading to a lower Δ/χ ratio and a higher neutral-effect threshold. Naloxone's life-saving effectiveness is meaningfully compromised only when Δ/χ exceeds 6.14, corresponding to an overdose rate below 0.0042577, at which point the optimal policy shifts to zero accessibility in both models. While no clear empirical evidence currently suggests that moral hazard reaches such extreme levels, this possibility cannot be entirely excluded, though under present real-world conditions, full naloxone accessibility likely remains the optimal policy.

7.3. Prospective Analysis: The Potential Emergence of Next-generation Ultra-potent Synthetic Opioids

We recognize that the continuous evolution of illicit opioids has resulted in increasingly potent and hazardous substances. As highlighted by the concern expressed in Section 5.1, the progression from traditional morphine to OxyContin (approximately 1.5 times more potent and widely regarded as a catalyst of the U.S. opioid crisis), followed by heroin (roughly twice as potent), and now fentanyl (50–100 times more potent), illustrates a clear pattern: each significant increase in potency has triggered a new wave of the epidemic, heightening overdose risks and intensifying public health challenges.

In this section, we further examine whether the FDA should proactively reassess its current policy of expanding naloxone accessibility, particularly in anticipation of future scenarios where the crisis may be driven by even more potent synthetic opioids—such as carfentanil (approximately 10,000 times stronger than morphine), ohmefentanyl (averaging 6,300 times more potent, with one isomer reaching up to 18,000 times (Yong et al. 2003)), or other similarly powerful analogs. These substances may substantially increase the overdose rate χ and reduce naloxone's effectiveness, as reflected by higher δ_l. On one hand, their high potential for physical dependence may lead to more severe withdrawal symptoms when use is curtailed; on the other hand, increased physiological tolerance may drive individuals to consume larger doses, further elevating overdose risk. Moreover, animal studies suggest that naloxone may fail to reverse carfentanil-induced overdoses, leaving individuals vulnerable to death, prolonged toxicity, and severe side effects (Langston et al. 2020).

Assuming no moral hazard, we retain the parameter estimates from Section 7.1 and focus on how changes in χ and δ_l influence the optimal policy. In the basic SAS model, it is well established that as long as naloxone provides even slight therapeutic benefit, full accessibility remains the optimal policy. However, the dynamics shift in the D-SAS model. As illustrated in Figure 9, the emergence of more potent and harmful opioids significantly alters the policy landscape. Notably, when both the overdose rate and the likelihood of severe withdrawal or increased use are high, the optimal policy shifts to zero accessibility (upper-right region of Figure 9) for FDA. For instance, if a potent opioid elevates the overdose rate χ to six times its original value and raises δ_l to 0.6 (black dot in Figure 9), the optimal level of accessibility drops to zero. Although we cannot definitively claim that the upper-right region of Figure 9 precisely reflects future scenarios, it is important to recognize that fentanyl already presents extreme risks, and the potency of carfentanil and ohmefentanyl far exceeds that of fentanyl. We therefore recommend that the FDA carefully reassess naloxone accessibility policies should these more dangerous opioids continue to proliferate.

When moral hazard is taken into account, the influence of more potent opioids on optimal policy becomes more nuanced. It is not immediately clear whether such substances would raise or lower the neutral effect threshold, as this depends on the relative changes in the overdose rate χ and the mortality rate under naloxone treatment δ_l. In addition, notice that more potent opioids may exacerbate moral hazard by increasing physiological dependence and reinforcing risky use patterns. But, in the SAS-M model without interaction terms, the optimal naloxone accessibility level remains at 1, provided that the moral hazard level stays below the neutral effect threshold associated with these stronger substances.

In contrast, for the D-SAS-M model, the optimal accessibility may be completely different. Figure 10 illustrates how the combination of more potent opioids and moral hazard affects accessibility decisions. For both plots, the lower regions of the upward-sloping black curve represent scenarios

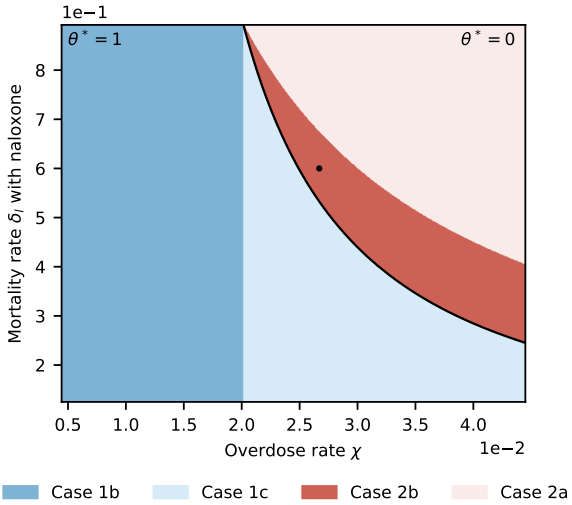

Figure 9 **The impact of increasingly potent opioids on the optimal naloxone accessibility policy in the D-SAS model. Each case shown in the legend corresponds to those defined in Theorem 2. Parameter values are based on the estimates derived in Section 7.1.**

where the neutral effect threshold exceeds the level of moral hazard, while the upper regions correspond to cases where the moral hazard level surpasses the threshold. Note that, if more potent opioids substantially reduce the effectiveness of naloxone in reversing overdoses, without causing a corresponding significant increase in the overdose rate (represented by the upper-left regions in both plots of Figure 10), the optimal policy shifts to zero accessibility. In such cases, expanding naloxone access may backfire, increasing overdose incidents under conditions of low survival likelihood.

Interestingly, when a highly potent and easily transmissible synthetic opioid results in both a significantly elevated overdose rate χ and a higher mortality rate even with naloxone administration δ_l (corresponding to the upper-right regions in both plots of Figure 10), the optimal policy for the FDA remains full naloxone accessibility ($\theta = 1$). This finding differs from the result observed in the D-SAS model, where full accessibility is not always optimal. Furthermore, we observe that as the level of moral hazard increases, the upper-right and upper-left regions expand, indicating that moral hazard has an increasingly pronounced effect on the structure of the optimal policy.

These findings together suggest that, in the presence of significant moral hazard and more lethal synthetic opioids, the FDA may need to revisit and reassess naloxone accessibility policies with heightened caution.

8. Conclusions and Future Directions

This paper examines a widely debated public health issue: the impact of expanded naloxone accessibility on the opioid epidemic—specifically, on overdose mortality. While some empirical studies

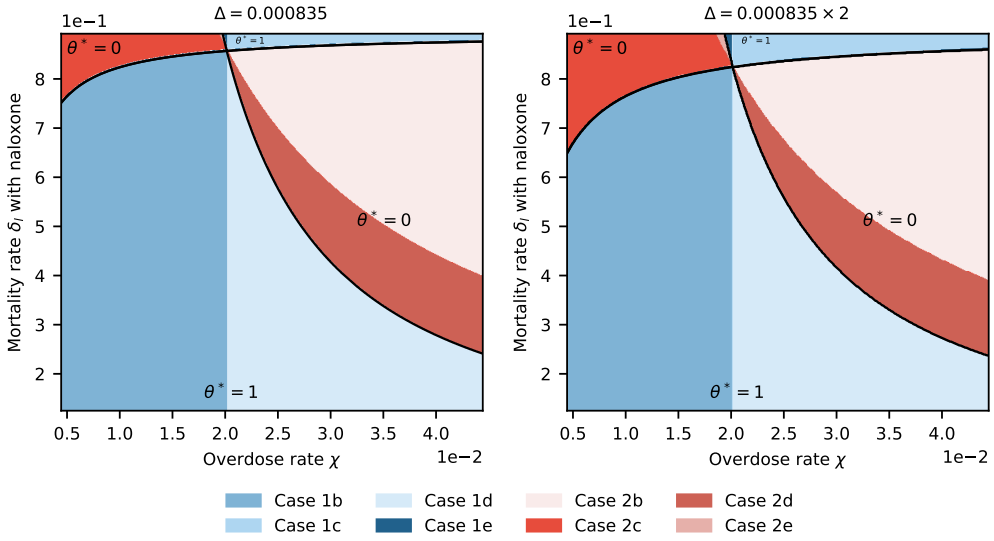

Figure 10 **The impact of increasingly potent opioids on the optimal naloxone accessibility policy in the D-SAS-M model. Each case shown in the legend corresponds to those defined in Theorem 3. Parameter values are provided in Section 7.1.**

suggest that broader naloxone access can unintentionally worsen the crisis through moral hazard, others emphasize its life-saving role in preventing overdose deaths. To inform this debate, we propose an analytical framework that characterizes optimal naloxone accessibility policies under varying epidemic conditions.

Summary of Optimal Naloxone Accessibility Across Models. We develop four progressively richer models, capturing the key epidemiological and behavioral dynamics of the opioid crisis. Across these models, we characterize how the structure of the optimal naloxone accessibility policy evolves:

- **SAS Model (Baseline):** In the absence of moral hazard or social contagion, full naloxone accessibility is always optimal.
- **SAS-M Model (Incorporating Moral Hazard):** Introducing moral hazard yields a bang-bang policy structure. Full accessibility is optimal when the behavioral response to naloxone (Δ) remains below a critical threshold; otherwise, no public accessibility is preferable.
- **D-SAS Model (Adding Social Contagion):** Peer-driven opioid misuse introduces additional complexity. Full accessibility remains optimal when transmission rates are low or naloxone is sufficiently effective, but under certain conditions, limited accessibility better mitigates mortality risks.
- **D-SAS-M Model (Moral Hazard and Social Contagion Combined):** The most comprehensive model retains the bang-bang policy structure, with optimal accessibility determined by the interaction between moral hazard, contagion dynamics, and naloxone effectiveness. Detailed conditions are summarized in Tables 2 and 3.

Policy Implications. Our analysis provides structured, transparent guidance for designing naloxone distribution policies that balance life-saving potential against unintended behavioral risks. First, the explicit policy thresholds derived in our model link empirical estimates of naloxone effectiveness and behavioral response to socially optimal access levels. This approach equips policymakers with a flexible decision-support tool that remains grounded in evolving evidence.

Second, the model highlights that while full accessibility is often optimal, especially in prescription-driven epidemics, emerging dynamics—such as social contagion or the proliferation of ultra-potent opioids like carfentanil—can fundamentally alter the optimal policy landscape. Notably, we show that the relationship between naloxone accessibility and overdose mortality may be non-monotonic, with moderate expansions in access potentially worsening outcomes before benefits materialize at higher access levels.

A calibrated case study based on U.S. data illustrates the framework's practical relevance. Under current epidemic conditions, full accessibility remains optimal, consistent with existing regulatory policies. However, this finding is conditional on present-day parameters; our results underscore that shifting epidemic dynamics, particularly increased opioid potency or intensified social transmission, may necessitate more restrictive or adaptive policies.

Importantly, even when the model recommends limited public accessibility ($\theta = 0$), naloxone remains available through medical channels, ensuring clinical use under professional judgment. Real-world policy decisions must therefore integrate naloxone access with complementary interventions—such as prevention, treatment expansion, and controlled prescribing—to holistically address the opioid crisis.

Future Research Directions. Several extensions can enhance the policy relevance and realism of our framework. First, while our analysis focuses on steady-state outcomes, policymakers often face short-term versus long-term trade-offs. For example, during overdose surges, reducing immediate mortality may take precedence, even if riskier behaviors increase future OUD prevalence. Extending the model to incorporate finite-horizon, dynamic, or time-varying policies would provide valuable insights for crisis management.

Second, accounting for the role of witnesses in naloxone administration would improve realism. Overdose reversal often depends on bystander availability, meaning that accessibility alone may overstate effective coverage (Ogeil et al. 2018).

Finally, cost-benefit analyses that incorporate both epidemiological outcomes and operational considerations are essential. For instance, recent efforts to deploy naloxone vending machines in Oklahoma were curtailed due to high costs and logistical challenges (2 News Oklahoma, 2024). Future work should integrate such economic and operational factors to inform sustainable, effective, and context-specific naloxone policies.

References

Abramson, A. 2021. Substance use during the pandemic. *Monitor on Psychology*, 52 (2), 22.

Adamopoulou, E., J. Greenwood, N. Guner, K. Kopecky. 2024. The role of friends in the opioid epidemic, (working paper).

Ansari, S., S. Enayati, R. Akhavan-Tabatabaei, J. Kapp. 2024. Curbing the opioid crisis: Optimal dynamic policies for preventive and mitigating interventions. *Decision Analysis*, 21 (3), 165-193.

Ardeljan, A.D., B. Fiedler, L. Fiedler, G.R. Luck, D.G. Maki, L. Clayton. 2023. Naloxone over the counter: Increasing opportunities and challenges for health providers. *The American Journal of Medicine*, 136 504-506.

Attari, I., J. Helm, J. Mejia. 2024. Hiding behind complexity: Supply chain, oversight, race, and the opioid crisis. *Production and Operations Management*, (forthcoming).

Battista, N., L. Pearcy, W. Strickland. 2019. Modeling the prescription opioid epidemic. *Bulletin of Mathematical Biology*, 81 2258-2289.

Baucum, M., M. Harris, L.e Kessler, G. Lu. 2025. Reducing overdose deaths and mitigating county disparities: Optimal allocation of substance use treatment centers. *Manufacturing & Service Operations Management*, 27 (3), 736-756.

Bertsimas, D., Digalakis J., A. Jacquillat, M. Li, A. Previero. 2022. Where to locate COVID-19 mass vaccination facilities? *Naval Research Logistics*, 69 (2), 179-200.

Bobroske, K., M. Freeman, L. Huan, A. Cattrell, S. Scholtes. 2022. Curbing the opioid epidemic at its root: The effect of provider discordance after opioid initiation. *Management Science*, 68 (3), 2003-2015.

Burris, S., L. Beletsky, C. Castagna, C. Coyle, C. Crowe, J. McLaughlin. 2009. Stopping an invisible epidemic: Legal issues in the provision of naloxone to prevent opioid overdose. *Drexel Law Review*, 1 273.

Cawley, J., D. Dragone. 2024. Harm reduction for addictive consumption: When does it improve health and when does it backfire? *Journal of Health Economics*, 98 102931.

Chehrazi, N., L. E Cipriano, E. Enns. 2019. Dynamics of drug resistance: Optimal control of an infectious disease. *Operations Research*, 67 (3), 619-650.

Chen, Z., G. Kong. 2023. Hospital admission, facility-based isolation, and social distancing: An SEIR model with constrained medical resources. *Production and Operations Management*, 32 (5), 1397-1414.

Cole, S., M.F. Olive, Wirkus S. 2024. The dynamics of heroin and illicit opioid use disorder, casual use, treatment, and recovery: A mathematical modeling analysis. *Mathematical Biosciences and Engineering*, 21 3165-3206.

Cole, S., S. Wirkus. 2022. Modeling the dynamics of heroin and illicit opioid use disorder, treatment, and recovery. *Bulletin of Mathematical Biology*, 84 (4), 48.

Dasgupta, N., L. Beletsky, D. Ciccarone. 2018. Opioid crisis: No easy fix to its social and economic determinants. *American Journal of Public Health*, 108 (2), 182-186.

Djilali, S., T. Touaoula, Sofiane E. Miri. 2017. A heroin epidemic model: Very general non linear incidence, treat-age, and global stability. *Acta Applicandae Mathematicae*, 152 171-194.

Doe-Simkins, M., E. Quinn, Z. Xuan, A. Sorensen-Alawad, H. Hackman, A. Ozonoff, A.Y. Walley. 2014. Overdose rescues by trained and untrained participants and change in opioid use among substance-using participants in overdose education and naloxone distribution programs: a retrospective cohort study. *BMC Public Health*, 14 1-11.

Doleac, J., A. Mukherjee. 2022. The effects of naloxone access laws on opioid abuse, mortality, and crime. *The Journal of Law and Economics*, 65 (2), 211-238.

Freiermuth, C., R. Ancona, J. Brown, B. Punches, S. Ryan, T. Ingram, M. Lyons. 2023. Evaluation of a large-scale health department naloxone distribution program: Per capita naloxone distribution and overdose morality. *Plos One*, 18 (8), 1-14.

Gan, K., Y. Tang, A. Scheller-Wolf, S. Tayur. 2025. Optimizing wearable devices in personalized opioid use disorder treatments under budget constraint, (working paper).

Gao, X., N. Kong, P. Griffin. 2024. Shortening emergency medical response time with joint operations of uncrewed aerial vehicles with ambulances. *Manufacturing & Service Operations Management*, 26 (2), 447-464.

Gökçınar, A., M. Çakanyıldırım, T. Price, M. Adams. 2022. Balanced opioid prescribing via a clinical trade-off: Pain relief vs. adverse effects of discomfort, dependence, and tolerance/hypersensitivity. *Decision Analysis*, 19 (4), 297-318.

Greene, J. 2018. Naloxone "moral hazard" debate pits economists against physicians. *Annals of Emergency Medicine*, 72 (2), A13-A16.

Haley, D.F., R. Saitz. 2020. The opioid epidemic during the COVID-19 pandemic. *JAMA*, 324 (16), 1615-1617.

Hardin, J., J. Seltzer, H. Galust, A. Deguzman, I. Campbell, N. Friedman, G. Wardi, R.F. Clark, D. Lasoff. 2024. Emergency department take-home naloxone improves access compared with pharmacy-dispensed naloxone. *The Journal of Emergency Medicine*, 66 (4), e457-e462.

Hethcote, H. 2000. The mathematics of infectious diseases. *SIAM review*, 42 (4), 599-653.

Houser, R. 2023. Expanding access to naloxone: A necessary step to curb the opioid epidemic. *Disaster Medicine and Public Health Preparedness*, 17 e245.

Huang, G., A. Liu. 2013. A note on global stability for a heroin epidemic model with distributed delay. *Applied Mathematics Letters*, 26 (7), 687-691.

Jakubowski, A., H. Kunins, Z. Huxley-Reicher, A. Siegler. 2018. Knowledge of the 911 good samaritan law and 911-calling behavior of overdose witnesses. *Substance Abuse*, 39 (2), 233-238.

Jawa, R., S. Murray, M. Tori, J. Bratberg, A. Walley. 2022. Federal policymakers should urgently and greatly expand naloxone access. *American Journal of Public Health*, 112 (4), 558-561.

Johnson, A., C. Cunningham, E. Arnold, W. Rosamond, J. Zègre-Hemsey. 2021. Impact of using drones in emergency medicine: What does the future hold? *Open Access Emergency Medicine*, 13 487-498.

Jones, C., B. Han, G. Baldwin, E. Einstein, W. Compton. 2023. Use of medication for opioid use disorder among adults with past-year opioid use disorder in the US, 2021. *JAMA Network Open*, 6 (8), e2327488-e2327488.

KC, D., T. Kim, J. Liu. 2022. Electronic prescription monitoring and the opioid epidemic. *Production and Operations Management*, 31 (11), 4057-4074.

Keyes, K., C. Rutherford, A. Hamilton, J. Barocas, K. Gelberg, P. Mueller, D. Feaster, N. El-Bassel, M. Cerdá. 2022. What is the prevalence of and trend in opioid use disorder in the United States from 2010 to 2019? Using multiplier approaches to estimate prevalence for an unknown population size. *Drug and Alcohol Dependence Reports*, 3 100052.

Kline, A., D. Mattern, N. Cooperman, P. Dooley-Budsock, J. Williams, S. Borys. 2020. "a blessing and a curse:" Opioid users' perspectives on naloxone and the epidemic of opioid overdose. *Substance Use & Misuse*, 55 (8), 1280-1287.

Kun, Á., A. Hubai, A. Král, J. Mokos, B. Mikulecz, Á. Radványi. 2023. Do pathogens always evolve to be less virulent? The virulence–transmission trade-off in light of the COVID-19 pandemic. *Biologia Futura*, 74 (1), 69-80.

Lambdin, B., R. Bluthenthal, J. Humphrey, P. LaKosky, S. Prohaska, A. Kral. 2023. 'new evidence' for syringe services programs? A call for rigor and skepticism. *International Journal of Drug Policy*, 121 104107.

Langston, J., M. Moffett, J. Makar, B. Burgan, T. Myers. 2020. Carfentanil toxicity in the African green monkey: Therapeutic efficacy of naloxone. *Toxicology Letters*, 325 34-42.

Lejeune, M., W. Ma. 2025. Drone-delivery network for Opioid overdose: Nonlinear integer queueing-optimization models and methods. *Operations Research*, 73 (1), 86-108.

Li, M., H. Bouardi, O. Lami, T. Trikalinos, N. Trichakis, D. Bertsimas. 2023. Forecasting COVID-19 and analyzing the effect of government interventions. *Operations Research*, 71 (1), 184-201.

Liu, J., A. Bharadwaj. 2020. Drug abuse and the internet: Evidence from craigslist. *Management Science*, 66 (5), 2040-2049.

Liu, Y., K. Xie, W. Chen. 2025. Recreational cannabis legalization and illicit drugs: Drug usage, mortality, and darknet transactions. *Production and Operations Management*, 34 (1), 99-119.

Luo, J., B. Stellato. 2024. Frontiers in operations: Equitable data-driven facility location and resource allocation to fight the opioid epidemic. *Manufacturing & Service Operations Management*, 26 (4), 1229-1244.

Luthar, S.S., S.F. Anton, K.R. Merikangas, B.J. Rounsaville. 1992. Vulnerability to drug abuse among opioid addicts' siblings: individual, familial, and peer influences. *Comprehensive Psychiatry*, 33 (3), 190-196.

Mars, S., P. Bourgois, G. Karandinos, F. Montero, D. Ciccarone. 2014. "every 'never'i ever said came true": Transitions from opioid pills to heroin injecting. *International Journal of Drug Policy*, 25 (2), 257-266.

Martcheva, M. 2015. *An introduction to mathematical epidemiology*, vol. 61. Springer.

Mehrez, A., A. Gafni. 1987. The optimal treatment strategy—a patient's perspective. *Management Science*, 33 (12), 1602-1612.

Messinger, J., L. Beletsky, A. Kesselheim, R. Barenie. 2023. Moving naloxone over the counter is necessary but not sufficient. *Annals of Internal Medicine*, 176 (8), 1109-1112.

Ogeil, R., J. Dwyer, L. Bugeja, C. Heilbronn, D. Lubman, B. Lloyd. 2018. Pharmaceutical opioid overdose deaths and the presence of witnesses. *International Journal of Drug Policy*, 55 8-13.

Ornato, J., A. You, G. McDiarmid, L. Keyser-Marcus, A. Surrey, J. Humble, S. Dukkipati, L. Harkrader, S. Davis, J. Moyer, D. Tidwell, M. Peberdy. 2020. Feasibility of bystander-administered naloxone delivered by drone to opioid overdose victims. *The American Journal of Emergency Medicine*, 38 (9), 1787-1791.

Packham, A. 2022. Syringe exchange programs and harm reduction: New evidence in the wake of the opioid epidemic. *Journal of Public Economics*, 215 104733.

Peltzman, S. 1975. The effects of automobile safety regulation. *Journal of Political Economy*, 83 (4), 677-725.

Pernell, K., J. Jung. 2024. Rethinking moral hazard: Government protection and bank risk-taking. *Socio-Economic Review*, 22 (2), 625-653.

Qayyum, S., R. Ansari, I. Ullah, D. Siblini. 2023. The FDA approves the second OTC naloxone–a step toward opioid crisis mitigation. *International Journal of Surgery*, 109 (12), 4349.

Rao, I., K. Humphreys, M. Brandeau. 2021. Effectiveness of policies for addressing the US opioid epidemic: A model-based analysis from the Stanford-Lancet commission on the north American opioid crisis. *The Lancet Regional Health–Americas*, 3 100031.

Rees, D.I., J.J. Sabia, L.M. Argys, J. Latshaw, D. Dave. 2017. With a little help from my friends: the effects of naloxone access and good samaritan laws on opioid-related deaths. Tech. rep., National Bureau of economic research.

Reider, B. 2019. Opioid epidemic. *The American Journal of Sports Medicine*, 47 (5), 1039-1042.

Rockett, M.L., H.K. Knudsen, C.B. Oser. 2024. The influence of familial networks and stigma on prison-based medication initiation for individuals with opioid use disorder: Clinicians' perceptions. *Journal of Substance Use and Addiction Treatment*, 162 209353.

Rzasa, L., J. Galinkin. 2018. Naloxone dosage for opioid reversal: Current evidence and clinical implications. *Therapeutic Advances in Drug Safety*, 9 (1), 63-88.

Saberi, S., S. Moore, S. Li, R. Mather, M. Daniels, A. Shahani, A. Barreveld, T. Griswold, P. McGuire, H. Connery. 2024. Systemized approach to equipping medical students with naloxone: a student-driven

initiative to combat the opioid crisis. *BMC Medical Education*, 24 (1), 241.

Sagberg, F., S. Fosser, I. Sætermo. 1997. An investigation of behavioural adaptation to airbags and antilock brakes among taxi drivers. *Accident Analysis & Prevention*, 29 (3), 293-302.

Spencer, N. 2023. Does drug decriminalization increase unintentional drug overdose deaths?: Early evidence from oregon measure 110. *Journal of Health Economics*, 91 102798.

Tse, W., F. Djordjevic, V. Borja, L. Picco, T. Lam, A. Olsen, S. Larney, P. Dietze, S. Nielsen. 2022. Does naloxone provision lead to increased substance use? A systematic review to assess if there is evidence of a 'moral hazard'associated with naloxone supply. *International Journal of Drug Policy*, 100 103513.

Wagner, K.D., T.W. Valente, M. Casanova, S.M. Partovi, B.M. Mendenhall, J.H. Hundley, M. Gonzalez, J.B. Unger. 2010. Evaluation of an overdose prevention and response training programme for injection drug users in the skid row area of Los Angeles, CA. *International Journal of Drug Policy*, 21 (3), 186-193.

Worsham, C.M., M.L. Barnett. 2020. The role of the household in prescription opioid safety. *JAMA Network Open*, 3 (3), e201108-e201108.

Yang, J., A. Mishra. 2025. Diversion in prescription opioid supply chains: Evidence from the drug supply chain security act. *Manufacturing & Service Operations Management*, 27 (3), 679-699.

Yong, Z., W. Hao, Y. Weifang, D. Qiyuan, C. Xinjian, J. Wenqiao, Z. Youcheng. 2003. Synthesis and analgesic activity of stereoisomers of cis-fluoro-ohmefentanyl. *Die Pharmazie-An International Journal of Pharmaceutical Sciences*, 58 (5), 300-302.

Zaric, G., M. Brandeau, P. Barnett. 2000. Methadone maintenance and HIV prevention: A cost-effectiveness analysis. *Management Science*, 46 (8), 1013-1031.

E-Companion: *Expanding Naloxone Accessibility: A Lifesaver or a Risky Setback?*

EC.1. Analysis of the D-SAS Model with Mass-Action Incidence $\beta S(t)A(t)$

The dynamics of the D-SAS model under mass action incidence, represented by the term $\beta S(t)A(t)$, are governed by the following system of differential equations:

$$\begin{cases} \dot{S}(t) = \Lambda - (\alpha+\eta)S(t) - \beta S(t)A(t) + \gamma A(t), \\ \dot{A}(t) = \eta S(t) + \beta S(t)A(t) - \chi\theta\delta_l A(t) - \chi(1-\theta)\delta_h A(t) - \alpha A(t) - \gamma A(t), \\ S(t) \geq 0, \quad A(t) \geq 0. \end{cases} \tag{EC.1.1}$$

Let $\rho = \alpha(\alpha+\gamma+\eta) - \beta\Lambda + \chi(\alpha+\eta)\left(\theta\delta_l + (1-\theta)\delta_h\right)$. The only feasible equilibrium point of system (EC.1.1) is given by:

$$(S_D^{m,*}, A_D^{m,*}) = \left(\frac{\rho + 2\beta\Lambda - \sqrt{4\beta\eta\Lambda(\alpha+\chi(\theta\delta_l+(1-\theta)\delta_h)) + \rho^2}}{2\alpha\beta}, \frac{\sqrt{4\beta\eta\Lambda(\alpha+\chi(\theta\delta_l+(1-\theta)\delta_h)) + \rho^2} - \rho}{2\beta(\alpha+\chi(\theta\delta_l+(1-\theta)\delta_h))} \right).$$

Given this equilibrium, our goal is to minimize the expected number of overdoses through an optimal accessibility policy:

$$\min_{\theta\in[0,1]} \quad \mathcal{D}_D^m(\theta) := \chi\left(\theta\delta_l + (1-\theta)\delta_h\right) A_D^{m,*}. \tag{EC.1.2}$$

To analyze this objective, we define the following expressions:

$$\begin{aligned} \mathcal{U}_h &= \alpha^2 - \beta\Lambda + \sqrt{\left(\alpha(\alpha+\gamma+\eta) - \beta\Lambda + \chi(\alpha+\eta)\delta_h\right)^2 + 4\beta\eta\Lambda(\alpha+\chi\delta_h)} + \alpha(\gamma+\eta), \\ \mathcal{V}_h &= \chi\delta_h \left(\frac{\beta\Lambda(\eta-\alpha) + \alpha(\alpha+\eta)(\alpha+\gamma+\eta) + \chi(\alpha+\eta)^2\delta_h}{\sqrt{\left(\alpha(\alpha+\gamma+\eta) - \beta\Lambda + \chi(\alpha+\eta)\delta_h\right)^2 + 4\beta\eta\Lambda(\alpha+\chi\delta_h)}} \right), \\ \mathcal{U}_l &= \alpha^2 - \beta\Lambda + \sqrt{\left(\alpha(\alpha+\gamma+\eta) - \beta\Lambda + \chi(\alpha+\eta)\delta_l\right)^2 + 4\beta\eta\Lambda(\alpha+\chi\delta_l)} + \alpha(\gamma+\eta), \\ \mathcal{V}_l &= \chi\delta_l \left(\frac{\beta\Lambda(\eta-\alpha) + \alpha(\alpha+\eta)(\alpha+\gamma+\eta) + \chi(\alpha+\eta)^2\delta_l}{\sqrt{\left(\alpha(\alpha+\gamma+\eta) - \beta\Lambda + \chi(\alpha+\eta)\delta_l\right)^2 + 4\beta\eta\Lambda(\alpha+\chi\delta_l)}} \right). \end{aligned}$$

THEOREM EC.1.1 **(Optimal Accessibility under Mass Action Incidence)**. *The solution to problem (EC.1.2) follows the structure below:*

1. ***Full accessibility*** $(\theta = 1)$ ***is optimal*** *if any of the following holds:*

a. $\beta\Lambda \leq \gamma(\alpha+\eta)$;

b. $\beta\Lambda > \gamma(\alpha+\eta)$ *and* $\mathcal{V}_h \leq \mathcal{U}_h$;

c. $\beta\Lambda > \gamma(\alpha+\eta)$, $\mathcal{V}_h > \mathcal{U}_h$, $\mathcal{V}_l < \mathcal{U}_l$, *and* $\mathcal{D}_D^m(\theta=1) \leq \mathcal{D}_D^m(\theta=0)$.

2. ***No accessibility*** $(\theta = 0)$ ***is optimal*** *if any of the following holds:*

a. $\beta\Lambda > \gamma(\alpha+\eta)$ *and* $\mathcal{V}_l \geq \mathcal{U}_l$;

b. $\beta\Lambda > \gamma(\alpha+\eta)$, $\mathcal{V}_h > \mathcal{U}_h$, $\mathcal{V}_l < \mathcal{U}_l$, *and* $\mathcal{D}_D^m(\theta=0) < \mathcal{D}_D^m(\theta=1)$.

While the specific conditions differ slightly from those in Theorem 2 under standard incidence $\beta S(t)A(t)/N(t)$, the overall structure of the solution and the key insights remain consistent.

EC.2. Equilibrium of the D-SAS and D-SAS-M Models

Let $\Omega=\sqrt{\zeta}$, where $\zeta=(\alpha-\beta+\gamma+\eta+\chi(1-\theta)\delta_h+\chi\theta\delta_l)^2+4\beta\eta>0$. There are two sets of solutions for equations

$$\begin{cases}\Lambda-(\alpha+\eta)\,S_D^*-\beta\dfrac{S_D^*A_D^*}{S_D^*+A_D^*}+\gamma A_D^*=0,\\ \eta S_D^*+\beta\dfrac{S_D^*A_D^*}{S_D^*+A_D^*}-(\alpha+\gamma+\chi\theta\delta_l+\chi(1-\theta)\delta_h)\,A_D^*=0,\end{cases}$$

including

$$\begin{aligned}S_{D,1}^*&=\frac{\alpha\Lambda\,(\alpha+\beta+\gamma+\eta-\Omega)-\Lambda\chi\,((\theta-1)\delta_h-\theta\delta_l)\,(\beta-\gamma+\eta+(\theta-1)\chi\delta_h-\Omega-\theta\chi\delta_l)}{2\,(\alpha^2\beta+\chi\,((\theta-1)\delta_h-\theta\delta_l)\,(\alpha(\alpha-\beta+\gamma+\eta)+\chi(\alpha+\eta)\,(\theta\delta_l-(\theta-1)\delta_h)))},\\ A_{D,1}^*&=\frac{2\eta\Lambda}{-(\theta-1)\chi(\alpha+2\eta)\delta_h+\alpha\,(\alpha-\beta+\gamma+\eta+\Omega)+\theta\chi(\alpha+2\eta)\delta_l};\\ S_{D,2}^*&=\frac{\Lambda\,(\alpha\,(\alpha+\beta+\gamma+\eta+\Omega)-\chi\,((\theta-1)\delta_h-\theta\delta_l)\,(\beta-\gamma+\eta+(\theta-1)\chi\delta_h+\Omega-\theta\chi\delta_l))}{2\,(\alpha^2\beta+\chi\,((\theta-1)\delta_h-\theta\delta_l)\,(\alpha(\alpha-\beta+\gamma+\eta)+\chi(\alpha+\eta)\,(\theta\delta_l-(\theta-1)\delta_h)))},\\ A_{D,2}^*&=\frac{2\eta\Lambda}{-(\theta-1)\chi(\alpha+2\eta)\delta_h+\alpha\,(\alpha-\beta+\gamma+\eta-\Omega)+\theta\chi(\alpha+2\eta)\delta_l}.\end{aligned}$$

Notice that

$$\frac{S_{D,2}^*}{A_{D,2}^*}=\frac{\alpha-\beta+\gamma-\eta+\delta_h(\chi-\theta\chi)-\Omega+\theta\chi\delta_l}{2\eta}<0 \text{ and } \frac{S_{D,1}^*}{A_{D,1}^*}=\frac{\alpha-\beta+\gamma-\eta+\delta_h(\chi-\theta\chi)+\Omega+\theta\chi\delta_l}{2\eta}>0$$

because of $(\alpha-\beta+\gamma+\eta-\theta\chi\delta_h+\chi\delta_h+\theta\chi\delta_l)^2-\zeta=-4\beta\eta<0$. Given that $S_{D,2}^*$ and $A_{D,2}^*$ have opposite signs, that pair cannot represent a biologically valid equilibrium. On the other hand, it is easy to see that $A_{D,1}^*>0$, and thus $S_{D,1}^*>0$ due to $\frac{S_{D,1}^*}{A_{D,1}^*}>0$. Hence, the only admissible equilibrium for D-SAS model is $\left(S_D^*,A_D^*\right)=\left(S_{D,1}^*,A_{D,1}^*\right)$.

Let $\Omega_M=\sqrt{\zeta_M}$, where $\zeta_M=(\alpha-\beta+\gamma+\eta+\chi(1-\theta)\delta_h+(\chi+\Delta)\theta\delta_l)^2+4\beta\eta>0$. Similarly, the only admissible equilibrium for D-SAS-M model is

$$\begin{aligned}S_{D,M}^*&=\frac{\alpha\Lambda\,(\alpha+\beta+\gamma+\eta-\Omega_M)+\Lambda\,((\theta-1)\chi\delta_h-\theta(\Delta+\chi)\delta_l)\,(-\beta+\gamma-\eta+\delta_h(\chi-\theta\chi)+\Omega_M+\theta(\Delta+\chi)\delta_l)}{2\,(\alpha^2\beta+((\theta-1)\chi\delta_h-\theta(\Delta+\chi)\delta_l)\,(\alpha(\alpha-\beta+\gamma+\eta)+(\alpha+\eta)\,(\delta_h(\chi-\theta\chi)+\theta(\Delta+\chi)\delta_l)))},\\ A_{D,M}^*&=\frac{2\eta\Lambda}{-(\theta-1)\chi(\alpha+2\eta)\delta_h+\alpha\,(\alpha-\beta+\gamma+\eta+\Omega_M)+\theta(\alpha+2\eta)(\Delta+\chi)\delta_l}.\end{aligned}$$

EC.3. The Impact of Moral Hazard on Overdose Mortality

We define

$$\begin{aligned}\mathcal{T}_1&=(\theta-1)\chi\delta_h+\mathcal{T}_2-\theta\chi\delta_l,\\ \mathcal{T}_2&=\sqrt{(\alpha-\beta+\gamma+\eta+\chi(1-\theta)\delta_h+\chi\theta\delta_l)^2+4\beta\eta},\\ \Delta^*&=\frac{2\eta(\alpha+\beta+\gamma)+(\alpha-\beta+\gamma)^2+\eta^2-2\chi(\alpha-\beta+\gamma+\eta)\,((\theta-1)\delta_h-\theta\delta_l)}{2\theta\delta_l(\beta-\alpha-\gamma-\eta)}.\end{aligned}$$

PROPOSITION EC.3.1 **(The Impact of Moral Hazard on Overdose Mortality)**. *For a fixed accessibility θ, we have:*

Case 1. When $\beta\le\eta+\alpha+\gamma$, $\mathcal{D}'_{D,M}(\Delta)>0$.

Case 2. When $\beta>\eta+\alpha+\gamma$,

a. When $\mathcal{T}_1\le 0$, $\mathcal{D}'_{D,M}(\Delta)<0$;

b. When $\mathcal{T}_1>0$, $\mathcal{D}'_{D,M}(\Delta)>0$ when $0<\Delta\le\Delta^*$ and $\mathcal{D}'_{D,M}(\Delta)<0$ when $\Delta>\Delta^*$.

Proposition EC.3.1 clearly demonstrates that moral hazard could decrease overdose mortality. Although moral hazard is typically viewed as harmful because it encourages riskier opioid use. However, in some cases, the resulting increase in overdose deaths may disrupt OUD transmission, ultimately reducing its long-term prevalence and fatalities.

EC.4. Parameter Estimations

Given the inherent challenges in directly observing and statistically quantifying $A(t)$, Keyes et al. (2022) employed three distinct calibration approaches to estimate the size of the U.S. OUD population from 2010 to 2019, aiming to mitigate potential underestimation of its true magnitude. In this study, we use the average of the three calibrated estimates reported by Keyes et al. (2022) as our estimate for $A(t)$.

The sequence $S(t)$ is subsequently obtained by subtracting the estimated OUD population from the total U.S. population for each corresponding year. Prior to estimating model parameters, we apply Gaussian kernel smoothing to all time series data to reduce potential noise and improve estimation accuracy.

For notational convenience, we define $t_0 = 2010$, $t_1 = 2011$, $\cdots$, $t_T = 2019$, and introduce the time index set $\mathbb{T}_T := \{t_1, t_2, \ldots, t_T\}$ $(T = 9)$.

EC.4.1. Estimations

Estimation of natual death rate α. Let $\mathbf{D}_\alpha(t)$ and $\mathbf{D}(t)$ denote the number of deaths unrelated and related to opioid overdose, respectively. Then we have $\mathbf{D}_\alpha(t) = \text{Total Deaths in Year } t - \mathbf{D}(t)$ for the SAS family of models. Next, we have a regression function:

$$\mathbf{D}_\alpha(t) = \alpha(S(t) + A(t)) = \alpha N(t),$$

where $N(t)$ is the total population in the U.S. in year t. By the least squares method, the corresponding loss function is

$$\min_{\alpha} \quad L(\alpha) = \sum_{t \in \mathbb{T}_T} \left(\mathbf{D}_\alpha(t) - \alpha N(t)\right)^2. \tag{EC.4.3}$$

By solving problem (EC.4.3), we obtain $\alpha = 0.0083$.

Estimation of overall mortality rate regarding opioid overdose. In the SAS and D-SAS models, the overall mortality rate due to opioid overdose, given by $\chi(1-\theta)\delta_h + \chi\theta\delta_l$, can be denoted as ϕ. In the SAS-M and D-SAS-M models, the overall mortality rate, accounting for the effect of moral hazard, is given by $\chi(1-\theta)\delta_h + \chi\theta\delta_l + \Delta\theta\delta_l$, and is likewise denoted by ϕ. Thus, the regression function

$$\mathbf{D}(t) = \phi A(t)$$

holds for all SAS family of models. By the least squares method, the corresponding loss function is

$$\min_{\alpha} \quad L(\phi) = \sum_{t \in \mathbb{T}_T} \left(\mathbf{D}(t) - \phi A(t)\right)^2. \tag{EC.4.4}$$

By solving problem (EC.4.4), we obtain $\phi = 0.0038$.

Estimation of tranmission rate β. By rearranging the discrete version of the D-SAS and D-SAS-M models, we have:

$$\begin{cases} \Lambda - \alpha S(t) + \gamma A(t) - S(t+1) + S(t) - \eta S(t) = \beta \dfrac{S(t)A(t)}{N(t)}, \\ A(t+1) - A(t) + (\alpha + \gamma + \phi) A(t) - \eta S(t) = \beta \dfrac{S(t)A(t)}{N(t)}. \end{cases}$$

Let

$$\begin{aligned} Y_1(t) &= \Lambda - \alpha S(t) + \gamma A(t) - S(t+1) + S(t) - \eta S(t), \\ Y_2(t) &= A(t+1) - A(t) + (\alpha + \gamma + \phi) A(t) - \eta S(t), \\ X(t) &= \frac{S(t)A(t)}{N(t)}. \end{aligned}$$

By the least squares method, the corresponding loss function is

$$\min_{\beta} \quad L(\beta) = \sum_{t \in \mathbb{T}_{T-1}} \sum_{i=1,2} (Y_i(t) - \beta X(t))^2. \tag{EC.4.5}$$

Notice that the time set in problem (EC.4.5) is $\mathbb{T}_{T-1}$ instead of $\mathbb{T}_T$ because applying a first-order difference to a time series results in the loss of one observation. Then, by solving problem (EC.4.5), we obtain $\beta = 0.036782$.

Note that in our linear estimations of parameters α, ϕ, and β, the associated p-values are all below 0.05, indicating that these estimates are statistically significant and valid.

EC.4.2. Model Validation

After calibrating all the parameters, we assess the goodness of fit for the SAS family of models by substituting the calibrated values into the system and regenerating the trajectories of $S(t)$ and $A(t)$. Table EC.1 below reports the mean absolute percentage error (MAPE) between the model-generated sequences and the corresponding training data for $S(t)$ and $A(t)$.

Table EC.1 MAPE results for the SAS family of models.

	$S(t)$	$A(t)$	$\mathbf{D}(t)$
SAS and SAS-M models	0.0073705	0.0885703	0.25271483
D-SAS and D-SAS-M models	0.0031949	0.0492427	0.21796289

We observe that all MAPE values are relatively small, indicating that the proposed SAS family of models can effectively capture the progression of the opioid crisis. In particular, we note that the MAPE values further decrease in the D-SAS and D-SAS-M models, which incorporate social interaction terms, compared to their counterparts without such terms. This, to some extent, highlights the critical role of social transmission in driving the dynamics of OUD.

We further conducted a back-testing analysis of overdose deaths by solving the SAS family of models. As shown in Table EC.1, although the MAPE for opioid-related mortality is relatively higher than those for the trajectories of $S(t)$ and $A(t)$, the predicted number of deaths remains within the same order of magnitude as the observed data. Therefore, we consider this level of error to be acceptable, especially given that a MAPE below 0.5 is widely regarded as indicative of a reasonable forecast (Chen et al. 2003).

EC.5. Parameters used in Numerical Examples

Please see Table EC.2, Table EC.3 and Table EC.4.

Table EC.2 **Parameter values used in Figure 5: $\eta = 0.001$, $\gamma = 0.01$, $\chi = 0.02$, $\alpha = 0.006$, $\beta = 0.025$, and $\Lambda = 200{,}000$.**

	δ_h	δ_l	ω_h	ω_l	$\beta - \alpha - \eta - \gamma$
Left plot	0.90	0.10	−0.000124	0.000132	0.008
Right plot	0.80	0.38	−9.2e−5	4.24e−5	0.008

Table EC.3 **Parameter values used in Figure 6: $\eta = 0.0003$, $\gamma = 0.016$, $\alpha = 0.006$, and $\Lambda = 200{,}000$.**

	β	$\beta - \alpha - \eta - \gamma$
Left plot	0.025	0.0027
Right plot	Less than $\alpha + \eta + \gamma = 0.0223$ suffices	< 0

Table EC.4 **Parameter values used in Figure 8: $\eta = 0.001$, $\gamma = 0.001$, $\alpha = 0.006$, $\beta = 0.025$, and $\Lambda = 200{,}000$.**

	δ_h	δ_l	χ	ω_h	$\omega_{l,M}$	$\bar{\Delta}$
Left plot (Case 1d)	0.85	0.15	0.0250	−0.00033	0.0002564	0.11666
Left plot (Case 2d)	0.85	0.15	0.0250	−0.00033	0.0001850	0.11666
Right plot (Case 2e)	0.55	0.40	0.0125	0.00016	−0.000189	0.00469
Right plot (Case 1e)	0.55	0.40	0.0125	0.00016	−0.000298	0.00469

EC.6. Proofs of Theoretical Results

Proof of Proposition 1. Recall that the steady-state mortality is given by

$$\mathcal{D}(\theta) = \frac{\eta\Lambda\left[(1-\theta)\chi\delta_h + \theta\chi\delta_l\right]}{\alpha(\alpha+\gamma+\eta) + \chi(\alpha+\eta)\left[\theta\delta_l - (\theta-1)\delta_h\right]}.$$

Differentiating with respect to θ, we obtain

$$\mathcal{D}'(\theta) = -\frac{\alpha\eta\Lambda\chi(\alpha+\gamma+\eta)(\delta_h-\delta_l)}{\left[\alpha(\alpha+\gamma+\eta) - (\theta-1)\chi(\alpha+\eta)\delta_h + \theta\chi(\alpha+\eta)\delta_l\right]^2} < 0,$$

since $\delta_h > \delta_l$.

Thus, the mortality function $\mathcal{D}(\theta)$ is strictly decreasing in θ, and the minimum is attained at $\theta^* = 1$. Q.E.D.

Proof of Theorem 1. Recall that

$$\mathcal{D}_M(\theta) = \frac{\eta\Lambda\left((1-\theta)\chi\delta_h + \theta(\Delta+\chi)\delta_l\right)}{\alpha(\alpha+\gamma+\eta) + (\alpha+\eta)\left(\delta_h(\chi-\theta\chi) + \theta(\Delta+\chi)\delta_l\right)}.$$

Then, we have

$$\mathcal{D}'_M(\theta) = -\frac{\alpha\eta\Lambda(\alpha+\gamma+\eta)\left(\chi\delta_h - (\Delta+\chi)\delta_l\right)}{\left(\alpha(\alpha+\gamma+\eta) - (\theta-1)\chi(\alpha+\eta)\delta_h + \theta(\alpha+\eta)(\Delta+\chi)\delta_l\right)^2},$$

where the sign of $\mathcal{D}'_M(\theta)$ depends on the sign of $\chi\delta_h - (\Delta+\chi)\delta_l$. When $\Delta < \bar{\Delta} = \frac{\chi(\delta_h-\delta_l)}{\delta_l}$, we have $(\chi\delta_h - (\Delta+\chi)\delta_l) > 0$ and thus $\theta^* = 1$. When $\Delta > \bar{\Delta}$, however, we get that $(\chi\delta_h - (\Delta+\chi)\delta_l) < 0$ and thus $\theta^* = 0$. In particular, when $\Delta = \bar{\Delta}$, $\mathcal{D}'_M(\theta) = 0$ and, therefore, any accessibility is optimal. For clarity and consistency, we directly set $\theta^* = 0$ in this case. Q.E.D.

Proof of Theorem 2. Recall that

$$A^*_D = \frac{2\eta\Lambda}{-(\theta-1)\chi(\alpha+2\eta)\delta_h + \alpha\left(\alpha-\beta+\gamma+\eta+\Omega\right) + \theta\chi(\alpha+2\eta)\delta_l},$$

where

$$\Omega = \sqrt{2\eta(\alpha+\beta+\gamma) + (\alpha-\beta+\gamma)^2 + \eta^2 - \chi\left((\theta-1)\delta_h - \theta\delta_l\right)\left(2(\alpha-\beta+\gamma+\eta) + \delta_h(\chi-\theta\chi) + \theta\chi\delta_l\right)}.$$

Then, we have

$$\mathcal{D}_D(\theta) = \frac{\left((1-\theta)\chi\delta_h + \theta\chi\delta_l\right)2\eta\Lambda}{-(\theta-1)\chi(\alpha+2\eta)\delta_h + \alpha\left(\alpha-\beta+\gamma+\eta+\Omega\right) + \theta\chi(\alpha+2\eta)\delta_l},$$

and

$$\mathcal{D}'_D(\theta) = \frac{P(\theta)}{\Omega\left(-(\theta-1)\chi(\alpha+2\eta)\delta_h + \alpha\left(\alpha-\beta+\gamma+\eta+\Omega\right) + \theta\chi(\alpha+2\eta)\delta_l\right)^2},$$

where $P(\theta) = -2\alpha\eta\Lambda\chi\left(\delta_h-\delta_l\right)\left(\theta\chi\delta_h - \chi\delta_h + \Omega - \theta\chi\delta_l\right)\left(\alpha-\beta+\gamma+\eta-\theta\chi\delta_h+\chi\delta_h+\Omega+\theta\chi\delta_l\right)$.

Next, we focus our attention on the derivative of $P(\theta)$:

$$P'(\theta) = \frac{2\alpha\eta\Lambda\chi^2\left(\delta_h-\delta_l\right)^2(\alpha-\beta+\gamma+\eta)\left(\alpha-\beta+\gamma+\eta-\theta\chi\delta_h+\chi\delta_h+\Omega+\theta\chi\delta_l\right)}{\Omega}.$$

Note that the term $(\alpha-\beta+\gamma+\eta-\theta\chi\delta_h+\chi\delta_h+\Omega+\theta\chi\delta_l)$ in the numerator in $P'(\theta)$ is strictly positive since

$$\Omega^2 - (\alpha-\beta+\gamma+\eta-\theta\chi\delta_h+\chi\delta_h+\theta\chi\delta_l)^2 = 4\beta\eta > 0.$$

Thus, the sign of $P'(\theta)$ only depends on the sign of $(\alpha-\beta+\gamma+\eta)$. We, therefore, consider the following three cases:

Case 1: If $\beta < \alpha+\gamma+\eta$, $P(\theta)$ monotonically increases.

Case 2: If $\beta = \alpha+\gamma+\eta$, $P(\theta)$ is a constant.

Case 3: If $\beta > \alpha+\gamma+\eta$, $P(\theta)$ monotonically decreases.

From the above three cases, we know that $\mathcal{D}'_D(\theta) = 0$ has at most one solution when $\beta \neq \alpha+\gamma+\eta$.

Next, we analyze each of the above cases separately.

Case 1. When $\beta < \alpha+\gamma+\eta$, then $P'(\theta) > 0$ and $P(\theta)$ is increasing. Note that

$$P(\theta=1) = 2\alpha\eta\Lambda\chi\left(\delta_h-\delta_l\right)\mathcal{Y}_1\mathcal{Y}_2,$$

where

$$\mathcal{Y}_1 = \left(\chi\delta_l - \sqrt{2\eta(\alpha+\beta+\gamma) + (\alpha-\beta+\gamma)^2 + \eta^2 + \chi\delta_l\left(2(\alpha-\beta+\gamma+\eta) + \chi\delta_l\right)}\right),$$

$$\mathcal{Y}_2 = \left(\alpha-\beta+\gamma+\eta+\sqrt{2\eta(\alpha+\beta+\gamma)+(\alpha-\beta+\gamma)^2+\eta^2+\chi\delta_l\left(2(\alpha-\beta+\gamma+\eta)+\chi\delta_l\right)}+\chi\delta_l\right).$$

It is easy to see that when $\beta < \alpha+\gamma+\eta$, then $\mathcal{Y}_1 < 0$. Additionally, because

$$\left(2\eta(\alpha+\beta+\gamma)+(\alpha-\beta+\gamma)^2+\eta^2+\chi\delta_h\left(2(\alpha-\beta+\gamma+\eta)+\chi\delta_h\right)\right)-\left(\alpha-\beta+\gamma+\eta+\chi\delta_h\right)^2 = 4\beta\eta > 0,$$

we have $\mathcal{Y}_2 > 0$. Therefore, $P(\theta=1) < 0$ and thus $P(\theta) < 0$ for $\theta \in [0,1]$. Thus, $\mathcal{D}_D(\theta)$ is decreasing and thereby, $\theta^* = 1$.

Case 2. When $\beta = \alpha+\gamma+\eta$, then $P(\theta)$ can be simplified to $-8\alpha\eta^2\Lambda\chi(\alpha+\gamma+\eta)(\delta_h-\delta_l) < 0$. In this case, $\mathcal{D}'_D(\theta) < 0$ and thus $\mathcal{D}_D(\theta)$ is decreasing and $\theta^* = 1$.

Case 3. When $\beta > \alpha+\gamma+\eta$, then $P'(\theta) < 0$ and thus $P(\theta)$ is decreasing. Note that in this case,

$$P(\theta=0) = 2\alpha\eta\Lambda\chi(\delta_h-\delta_l)\mathcal{X}_1\mathcal{X}_2,$$

where

$$\begin{aligned}
\mathcal{X}_1 &= \left(\chi\delta_h-\sqrt{2\eta(\alpha+\beta+\gamma)+(\alpha-\beta+\gamma)^2+\eta^2+\chi\delta_h\left(2(\alpha-\beta+\gamma+\eta)+\chi\delta_h\right)}\right),\\
\mathcal{X}_2 &= \left(\alpha-\beta+\gamma+\eta+\sqrt{2\eta(\alpha+\beta+\gamma)+(\alpha-\beta+\gamma)^2+\eta^2+\chi\delta_h\left(2(\alpha-\beta+\gamma+\eta)+\chi\delta_h\right)}+\chi\delta_h\right).
\end{aligned} \tag{EC.6.6}$$

Importantly, even when $\beta > \alpha+\gamma+\eta$, then $\mathcal{X}_2, \mathcal{Y}_2 \geq 0$, because

$$\left(2\eta(\alpha+\beta+\gamma)+(\alpha-\beta+\gamma)^2+\eta^2+\chi\delta_h\left(2(\alpha-\beta+\gamma+\eta)+\chi\delta_h\right)\right)-\left(\alpha-\beta+\gamma+\eta+\chi\delta_h\right)^2 = 4\beta\eta > 0;$$

$$\left(2\eta(\alpha+\beta+\gamma)+(\alpha-\beta+\gamma)^2+\eta^2+\chi\delta_l\left(2(\alpha-\beta+\gamma+\eta)+\chi\delta_l\right)\right)-\left(\alpha-\beta+\gamma+\eta+\chi\delta_l\right)^2 = 4\beta\eta > 0.$$

Now there could be three cases:

Case 3.1. When $P(\theta=0) < 0$ (i.e., $\mathcal{X}_1 < 0 \Leftrightarrow \omega_h = (\alpha-\beta+\gamma+\eta)^2+4\beta\eta+2\chi\delta_h(\alpha-\beta+\gamma+\eta) > 0$), then $\mathcal{D}_D(\theta)$ is decreasing and thus $\theta^* = 1$.

Case 3.2. When $P(\theta=0) > 0$ and $P(\theta=1) < 0$ (i.e., $\mathcal{X}_1 > 0$ and $\mathcal{Y}_1 < 0 \Leftrightarrow \omega_h < 0$ and $\omega_l = (\alpha-\beta+\gamma+\eta)^2+4\beta\eta+2\chi\delta_l(\alpha-\beta+\gamma+\eta) > 0$), $\mathcal{D}(\theta)$ first increases and then decreases over the interval $[0,1]$. Thus, $\theta^* = \arg\min_{\theta\in\{0,1\}}\mathcal{D}_D(\theta)$ considering that the optimal solution can only exist at the extreme values. Note that when $\mathcal{D}_{D,M}(\theta=0) = \mathcal{D}_{D,M}(\theta=1)$, we set $\theta^* = 0$ for convenience.

Case 3.3. When $P(\theta=1) > 0$ (i.e., $\mathcal{Y}_1 > 0 \Leftrightarrow \omega_l < 0$), $\mathcal{D}_D(\theta)$ is increasing and thus $\theta^* = 0$.

Collecting the conditions under which $\theta^* = 1$ and $\theta^* = 0$ yields the desired characterization as stated. Q.E.D.

Proof of Theorem 3. We begin by examining the special case where $\Delta = \bar{\Delta}$. In this case, the D-SAS-M model becomes independent of the accessibility level θ, as the life-saving benefits of naloxone exactly offset the negative impact of moral hazard. The optimal solution is therefore not unique and may lie anywhere in the interval $[0,1]$. For consistency with the rest of the analysis, we adopt zero accessibility as the default choice.

We now proceed under the assumption that $\Delta \neq \bar{\Delta}$. Recall that

$$A^*_{D,M} = \frac{2\eta\Lambda}{-(\theta-1)\chi(\alpha+2\eta)\delta_h+\alpha(\alpha-\beta+\gamma+\eta+\Omega_M)+\theta(\alpha+2\eta)(\Delta+\chi)\delta_l},$$

where

$$\Omega_M = \sqrt{(\alpha-\beta+\gamma+\eta+\chi(1-\theta)\delta_h+(\chi+\Delta)\theta\delta_l)^2+4\beta\eta}.$$

Then, we have

$$\mathcal{D}_{D,M}(\theta) = \frac{2\eta\Lambda((1-\theta)\chi\delta_h + \theta(\Delta+\chi)\delta_l)}{-(\theta-1)\chi(\alpha+2\eta)\delta_h + \alpha\left(\alpha-\beta+\gamma+\eta+\Omega_M\right) + \theta(\alpha+2\eta)(\Delta+\chi)\delta_l}, \tag{EC.6.7}$$

and

$$\mathcal{D}'_{D,M}(\theta) = \frac{Q(\theta)}{\Omega_M\left(-(\theta-1)\chi(\alpha+2\eta)\delta_h + \alpha\left(\alpha-\beta+\gamma+\eta+\Omega_M\right) + \theta(\alpha+2\eta)(\Delta+\chi)\delta_l\right)^2},$$

where

$$Q(\theta) = -2\alpha\eta\Lambda\left(\chi\delta_h - (\Delta+\chi)\delta_l\right)\left((\theta-1)\chi\delta_h + \Omega_M - \theta(\Delta+\chi)\delta_l\right)\left(\alpha-\beta+\gamma+\eta+\delta_h(\chi-\theta\chi) + \Omega_M + \theta(\Delta+\chi)\delta_l\right).$$

Therefore,

$$Q'(\theta) = \frac{2\alpha\eta\Lambda(\alpha-\beta+\gamma+\eta)\left(\chi\delta_h - (\Delta+\chi)\delta_l\right)^2\left(\alpha-\beta+\gamma+\eta+\delta_h(\chi-\theta\chi) + \Omega_M + \theta(\Delta+\chi)\delta_l\right)}{\Omega_M},$$

$$Q(\theta=0) = 2\alpha\eta\Lambda\left(\chi\delta_h - (\Delta+\chi)\delta_l\right)\mathcal{X}_1\mathcal{X}_2,$$

$$Q(\theta=1) = 2\alpha\eta\Lambda\left(\chi\delta_h - (\Delta+\chi)\delta_l\right)\mathcal{Y}_{1,M}\mathcal{Y}_{2,M},$$

where $\mathcal{X}_1$ and $\mathcal{X}_2$ are defined in (EC.6.6) as well as

$$\mathcal{Y}_{1,M} = \left(-\sqrt{2\eta(\alpha+\beta+\gamma) + (\alpha-\beta+\gamma)^2 + \eta^2 + (\Delta+\chi)\delta_l\left(2(\alpha-\beta+\gamma+\eta) + (\Delta+\chi)\delta_l\right)} + (\Delta+\chi)\delta_l\right),$$

$$\mathcal{Y}_{2,M} = \left(\alpha-\beta+\gamma+\eta + \sqrt{2\eta(\alpha+\beta+\gamma) + (\alpha-\beta+\gamma)^2 + \eta^2 + (\Delta+\chi)\delta_l\left(2(\alpha-\beta+\gamma+\eta) + (\Delta+\chi)\delta_l\right)} + (\Delta+\chi)\delta_l\right) > 0.$$

Since $Q'(\theta)=0$ if and only if $\Delta=\bar{\Delta}$, provided that $\alpha-\beta+\gamma+\eta\neq 0$, the sign of $Q'(\theta)$ depends solely on the sign of $(\alpha-\beta+\gamma+\eta)$. We therefore consider the following cases:

Case 1: If $\beta<\alpha+\gamma+\eta$, then $Q(\theta)$ monotonically increases.

Case 2: If $\beta=\alpha+\gamma+\eta$, then $Q(\theta)$ is a constant.

Case 3: If $\beta>\alpha+\gamma+\eta$, then $Q(\theta)$ monotonically decreases.

From the three cases above, it follows that $\mathcal{D}'_{D,M}(\theta)=0$ has at most one solution when $\beta\neq\alpha+\gamma+\eta$.

Next, we analyze each of the above cases.

Case 1. When $\beta<\alpha+\gamma+\eta$, then $Q'(\theta)>0$ so $Q(\theta)$ is increasing. In this case, we have $\mathcal{X}_1,\mathcal{Y}_{1,M}<0$ and $\mathcal{X}_2,\mathcal{Y}_{2,M}>0$. Thus, the sign of $Q(\theta=0)$ and $Q(\theta=1)$ also depends on the sign of $(\chi\delta_h-(\Delta+\chi)\delta_l)$. There could be two cases:

Case 1.1. When $\Delta<\bar{\Delta}$, we have $Q(\theta=0),Q(\theta=1)<0$. Thus $\mathcal{D}'_{D,M}(\theta)<0$ and $\theta^*=1$.

Case 1.2. When $\Delta>\bar{\Delta}$, we have $Q(\theta=0),Q(\theta=1)>0$. Thus, $\mathcal{D}'_{D,M}(\theta)>0$ and $\theta^*=0$.

Case 2. When $\beta=\alpha+\gamma+\eta$, then $Q(\theta)$ is reduced to $-8\alpha\eta^2\Lambda(\alpha+\gamma+\eta)\left(\chi\delta_h-(\Delta+\chi)\delta_l\right)$. There could be two cases:

Case 2.1. When $\Delta<\bar{\Delta}$, we have $Q(\theta)<0$. Thus, $\mathcal{D}'_{D,M}(\theta)<0$ and $\theta^*=1$.

Case 2.2. When $\Delta>\bar{\Delta}$, we have $Q(\theta)>0$. Thus, $\mathcal{D}'_{D,M}(\theta)>0$ and $\theta^*=0$.

Case 3. When $\beta>\alpha+\gamma+\eta$, $Q'(\theta)<0$ and thus $Q(\theta)$ is decreasing. There could be three cases:

Case 3.1. When $Q(\theta=0)\leq 0$:

Case 3.1.1. When $\Delta<\bar{\Delta}$ and $\mathcal{X}_1<0$ (i.e., $\omega_h=(\alpha-\beta+\gamma+\eta)^2+4\beta\eta+2\chi\delta_h(\alpha-\beta+\gamma+\eta)>0$), we have $Q(\theta)<0$ for all $\theta\in[0,1]$. Thus, $\mathcal{D}'_{D,M}(\theta)<0$ and $\theta^*=1$.

Case 3.1.2. When $\Delta>\bar{\Delta}$ and $\mathcal{X}_1>0$ (i.e., $\omega_h<0$), we have $Q(\theta)<0$ for all $\theta\in[0,1]$. Thus, $\mathcal{D}'_{D,M}(\theta)<0$ and $\theta^*=1$.

Case 3.1.3. When $\mathcal{X}_1 = 0$ (i.e., $\omega_h = 0$), we have $Q(\theta = 0) = 0$ and $Q(\theta) < 0$ for all $\theta \in (0, 1]$. Thus, $\theta^* = 1$.

Case 3.2. When $Q(\theta = 0) > 0$ and $Q(\theta = 1) < 0$, then $\mathcal{D}_{D,M}(\theta)$ first increases and then decreases over the interval $[0, 1]$:

Case 3.2.1. When $\Delta < \bar{\Delta}$, $\mathcal{X}_1 > 0$ (i.e., $\omega_h < 0$) and $\mathcal{Y}_{1,M} < 0$ (i.e., $\omega_{l,M} = (\alpha - \beta + \gamma + \eta)^2 + 4\beta\eta + 2(\chi + \Delta)\delta_l(\alpha - \beta + \gamma + \eta) > 0$), $\theta^* = \arg\min_{\theta \in \{0,1\}} \mathcal{D}_{D,M}(\theta)$ because, in this case, the optimal solution exists only on the boundaries.

Case 3.2.2. When $\Delta > \bar{\Delta}$, $\mathcal{X}_1 < 0$ (i.e., $\omega_h > 0$) and $\mathcal{Y}_{1,M} > 0$ (i.e., $\omega_{l,M} < 0$), $\theta^* = \arg\min_{\theta \in \{0,1\}} \mathcal{D}_{D,M}(\theta)$ because, in this case, the optimal solution exists only on the boundaries.

Note that when $\mathcal{D}_{D,M}(\theta = 0) = \mathcal{D}_{D,M}(\theta = 1)$, we set $\theta^* = 0$ for convenience.

Case 3.3. When $Q(\theta = 1) \geq 0$:

Case 3.3.1. When $\Delta < \bar{\Delta}$ and $\mathcal{Y}_{1,M} > 0$ (i.e., $\omega_{l,M} < 0$), we have $Q(\theta) > 0$ for all $\theta \in [0, 1]$. Thus, $\mathcal{D}'_{D,M}(\theta) < 0$ and $\theta^* = 0$.

Case 3.3.2. When $\Delta > \bar{\Delta}$ and $\mathcal{Y}_{1,M} < 0$ (i.e., $\omega_{l,M} > 0$), we have $Q(\theta) > 0$ for all $\theta \in [0, 1]$. Thus, $\mathcal{D}'_{D,M}(\theta) < 0$ and $\theta^* = 0$.

Case 3.3.3. When $\mathcal{Y}_{1,M} = 0$ (i.e., $\omega_{l,M} = 0$), we have $Q(\theta = 1) = 0$ and $Q(\theta) > 0$ for all $\theta \in (0, 1]$. Thus, $\theta^* = 0$.

Collecting the conditions under which $\theta^* = 1$ and $\theta^* = 0$ yields the desired characterization stated. Q.E.D.

Proof of Theorem EC.1.1. The full expression of $\mathcal{D}_D^m(\theta)$ is

$$\mathcal{D}_D^m(\theta) = \frac{2\eta\Lambda\left(\delta_h(\chi - \theta\chi) + \theta\chi\delta_l\right)}{\rho + \sqrt{\rho^2 + 4\beta\eta\Lambda\left(\alpha + \delta_h(\chi - \theta\chi) + \theta\chi\delta_l\right)}},$$

and

$$\mathcal{D}_D^{'m}(\theta) = \frac{\mathcal{P}(\theta)}{\left(\rho + \sqrt{\rho^2 + 4\beta\eta\Lambda\left(\alpha + \delta_h(\chi - \theta\chi) + \theta\chi\delta_l\right)}\right)^2},$$

where

$$\begin{aligned}\mathcal{P}(\theta) = &-2\eta\Lambda\chi\left(\delta_h - \delta_l\right)\left(\rho + \sqrt{\rho^2 + 4\beta\eta\Lambda\left(\alpha + \chi(\theta\delta_l + (1-\theta)\delta_h)\right)}\right) \\ &+ 2\eta\Lambda\chi\left(\delta_h - \delta_l\right)\left(\chi(\theta\delta_l + (1-\theta)\delta_h)\left(\eta + \alpha + \frac{\beta\Lambda(\eta - \alpha) + \alpha(\alpha + \eta)(\alpha + \gamma + \eta) + \chi(\alpha + \eta)^2(\theta\delta_l + (1-\theta)\delta_h)}{\sqrt{\rho^2 + 4\beta\eta\Lambda\left(\alpha + \chi(\theta\delta_l + (1-\theta)\delta_h)\right)}}\right)\right).\end{aligned}$$

Additionally, we have

$$\mathcal{P}(\theta = 0) = 2\eta\Lambda\chi(\delta_h - \delta_l)(\mathcal{V}_h - \mathcal{U}_h),\ \mathcal{P}(\theta = 1) = 2\eta\Lambda\chi(\delta_h - \delta_l)(\mathcal{V}_l - \mathcal{U}_l),\ \text{and}$$

$$\mathcal{P}'(\theta) = \frac{8\alpha\beta\eta^2\Lambda^2\chi^3\left(\delta_h - \delta_l\right)^2\left((1-\theta)\delta_h + \theta\delta_l\right)\left(\alpha\gamma - \beta\Lambda + \gamma\eta\right)}{\left(\rho^2 + 4\beta\eta\Lambda\left(\alpha + \delta_h(\chi - \theta\chi) + \theta\chi\delta_l\right)\right)^{3/2}}.$$

Note that the sign of $\mathcal{P}'(\theta)$ only depends on the sign of $(\alpha\gamma - \beta\Lambda + \gamma\eta)$ because both the denominator of $\mathcal{P}'(\theta)$ and $8\alpha\beta\eta^2\Lambda^2\chi^3\left(\delta_h - \delta_l\right)^2\left((1-\theta)\delta_h + \theta\delta_l\right)$ are all greater than 0. We, therefore, consider the following cases:

Case 1: If $\beta\Lambda < \alpha\gamma + \gamma\eta$, then $\mathcal{P}(\theta)$ monotonically increases.

Case 2: If $\beta\Lambda = \alpha\gamma + \gamma\eta$, then $\mathcal{P}(\theta)$ is a constant.

Case 3: If $\beta\Lambda > \alpha\gamma + \gamma\eta$, then $\mathcal{P}(\theta)$ monotonically decreases.

From the above three cases, we know that $\mathcal{D}_D^{'m}(\theta) = 0$ has at most one solution when $\beta\Lambda \neq \alpha\gamma + \gamma\eta$.

Next, we analyze each of the above cases.

Case 1. When $\beta\Lambda < \alpha\gamma + \gamma\eta$, we first define

$$\mathcal{A} = \alpha(\alpha+\gamma+\eta), \quad \mathcal{C} = \beta\Lambda(\eta-\alpha) + \alpha(\alpha+\eta)(\alpha+\gamma+\eta),$$
$$\mathcal{E} = \sqrt{\alpha^2(\alpha+\gamma+\eta)^2 - 2\alpha\beta\Lambda(\alpha+\gamma-\eta) + \beta^2\Lambda^2 + \chi\delta_l\left(2\beta\Lambda(\eta-\alpha) + 2\alpha(\alpha+\eta)(\alpha+\gamma+\eta) + \chi(\alpha+\eta)^2\delta_l\right)},$$
$$\mathcal{F} = \chi\delta_l\left(2\beta\Lambda(\eta-\alpha) + 2\alpha(\alpha+\eta)(\alpha+\gamma+\eta) + \chi\delta_l((\alpha+\eta)(\alpha+\gamma+\eta) - \beta\Lambda)\right)$$
$$= \chi\delta_l\left(2\mathcal{C} + \chi\delta_l((\alpha+\eta)(\alpha+\gamma+\eta) - \beta\Lambda)\right).$$

Note that $\mathcal{C} > 0$ because $\mathcal{C} > (\alpha\gamma+\gamma\eta)(\eta-\alpha) + \alpha(\alpha+\eta)(\alpha+\gamma+\eta) = (\alpha+\eta)\left(\alpha^2+\alpha\eta+\gamma\eta\right) > 0$ when $\alpha > \eta$ and $\mathcal{C}$ must be more than 0 when $\alpha \leq \eta$. Additionally, we have $\mathcal{F} > 0$ because

$$\mathcal{F} > \chi\delta_l\left(2\mathcal{C} + \chi\delta_l((\alpha+\eta)(\alpha+\gamma+\eta) - \gamma(\alpha+\eta))\right) = \chi\delta_l\left(2\mathcal{C} + \chi\delta_l(\alpha+\eta)^2\right) > 0.$$

Next, we have

$$\mathcal{V}_l - \mathcal{U}_l = \frac{-(\mathcal{A}-\beta\Lambda)^2 + (\beta\Lambda-\mathcal{A})\mathcal{E} - \chi\delta_l\mathcal{C} - 4\alpha\beta\Lambda\eta}{\sqrt{\left(\alpha(\alpha+\gamma+\eta) - \beta\Lambda + \chi(\alpha+\eta)\delta_l\right)^2 + 4\beta\eta\Lambda\left(\alpha+\chi\delta_l\right)}}.$$

Since $-(\mathcal{A}-\beta\Lambda)^2 - \chi\delta_l\mathcal{C} - 4\alpha\beta\Lambda\eta < 0$ and

$$\begin{aligned}
&\left(-(\mathcal{A}-\beta\Lambda)^2 - \chi\delta_l\mathcal{C} - 4\alpha\beta\Lambda\eta\right)^2 - \left((\beta\Lambda-\mathcal{A})\mathcal{E}\right)^2 \\
=&4\alpha\beta\eta\Lambda\left(\alpha^2(\alpha+\gamma+\eta)^2 - 2\alpha\beta\Lambda(\alpha+\gamma-\eta) + \beta^2\Lambda^2 + \mathcal{F}\right) \\
=&4\alpha\beta\eta\Lambda\left(\alpha^2(\alpha+\gamma+\eta)^2 - 2\alpha\beta\Lambda(\alpha+\gamma+\eta) + \beta^2\Lambda^2 + 4\alpha\beta\Lambda\eta + \mathcal{F}\right) \\
=&4\alpha\beta\eta\Lambda\left((\mathcal{A}-\beta\Lambda)^2 + 4\alpha\beta\Lambda\eta + \mathcal{F}\right) > 0,
\end{aligned}$$

we obtain that $\mathcal{V}_l - \mathcal{U}_l < 0$ and thus, $\mathcal{P}(\theta=1) < 0$. Consequently, $\mathcal{D}_D^{'m}(\theta) < 0$ and $\theta^* = 1$.

Case 2: When $\beta\Lambda = \alpha\gamma + \gamma\eta$, then $P(\theta)$ can be reduced to

$$\mathcal{P}(\theta) = -4\eta\Lambda\chi(\alpha+\eta)\alpha\left(\delta_h - \delta_l\right) < 0.$$

Thus, $\mathcal{D}_D^{'m}(\theta) < 0$ and $\theta^* = 1$.

Case 3: When $\beta\Lambda > \alpha\gamma + \gamma\eta$:

Case 3.1: When $\mathcal{P}(\theta=1) \geq 0$ (i.e., $\mathcal{V}_l \geq \mathcal{U}_l$), then $\mathcal{P}(\theta) \geq 0$ for $\theta \in [0,1]$. Thus, $\mathcal{D}_D^{'m}(\theta) \geq 0$ and $\theta^* = 0$.

Case 3.2: When $\mathcal{P}(\theta=0) > 0$ and $\mathcal{P}(\theta=1) < 0$ (i.e., $\mathcal{V}_l < \mathcal{U}_l$ and $\mathcal{V}_h > \mathcal{U}_h$), then $\mathcal{P}(\theta)$ has a unique root between 0 and 1, which means that $\mathcal{D}_M^m(\theta)$ first increases and then decrease over the interval $[0,1]$. Thus, $\theta^* = \arg\min_{\theta\in\{0,1\}} \mathcal{D}_M^m(\theta)$ considering that the optimal solution can only exist on the boundaries. Note that when $\mathcal{D}_M^m(\theta=0) = \mathcal{D}_M^m(\theta=1)$, we set $\theta^* = 0$ for convenience.

Case 3.3: When $\mathcal{P}(\theta=0) \leq 0$ (i.e., $\mathcal{V}_h \leq \mathcal{U}_h$), then $P(\theta) \leq 0$ for $\theta \in [0,1]$. Thus, $\mathcal{D}_D^{'m}(\theta) \leq 0$ and $\theta^* = 1$.

Collecting the conditions under which $\theta^* = 1$ and $\theta^* = 0$ yields the desired characterization stated. Q.E.D.

Proof of Proposition EC.3.1. In (EC.6.7), we have obtained

$$\mathcal{D}_{D,M} = \frac{2\eta\Lambda((1-\theta)\chi\delta_h + \theta(\Delta+\chi)\delta_l)}{-(\theta-1)\chi(\alpha+2\eta)\delta_h + \alpha\left(\alpha-\beta+\gamma+\eta+\Omega_M\right) + \theta(\alpha+2\eta)(\Delta+\chi)\delta_l},$$

where

$$\Omega_M = \sqrt{(\alpha-\beta+\gamma+\eta+\chi(1-\theta)\delta_h + (\chi+\Delta)\theta\delta_l)^2 + 4\beta\eta}.$$

For a fixed θ, we have

$$\mathcal{D}'_{D,M}(\Delta) = \frac{\mathcal{L}(\Delta)}{\Omega_M\left(-(\theta-1)\chi(\alpha+2\eta)\delta_h + \alpha\left(\alpha-\beta+\gamma+\eta+\Omega_M\right) + \theta(\alpha+2\eta)(\Delta+\chi)\delta_l\right)^2},$$

where

$$\mathcal{L}(\Delta) = 2\alpha\eta\theta\Lambda\delta_l\left(\theta\chi\delta_h - \chi\delta_h + \Omega_M - \Delta\theta\delta_l - \theta\chi\delta_l\right)\left(\alpha-\beta+\gamma+\eta-\theta\chi\delta_h + \chi\delta_h + \Omega_M + \Delta\theta\delta_l + \theta\chi\delta_l\right).$$

Next, we have

$$\mathcal{L}'(\Delta) = \frac{2\alpha\eta\theta^2\Lambda\delta_l^2(\alpha-\beta+\gamma+\eta)\left(\alpha-\beta+\gamma+\eta-\theta\chi\delta_h + \chi\delta_h + \Omega_M + \Delta\theta\delta_l + \theta\chi\delta_l\right)}{\Omega_M}.$$

Note that $(\alpha-\beta+\gamma+\eta-\theta\chi\delta_h + \chi\delta_h + \Omega_M + \Delta\theta\delta_l + \theta\chi\delta_l) > 0$, and thus the sign of $\mathcal{L}'(\Delta)$ only depends on the sign of $(\alpha-\beta+\gamma+\eta)$. We, therefore, consider the following cases:

Case 1: If $\beta \le \alpha+\gamma+\eta$, then $\mathcal{L}(\Delta)$ monotonically increases.

Case 2: If $\beta > \alpha+\gamma+\eta$, then $\mathcal{L}(\Delta)$ monotonically decreases.

From the above three cases, we know that $\mathcal{D}'_{D,M}(\Delta) = 0$ has at most one solution when $\beta \neq \alpha+\gamma+\eta$. Next, we analyze each of the above cases.

Case 1. When $\beta \le \alpha+\gamma+\eta$, there are two cases.

Case 1.1. When $\beta < \alpha+\gamma+\eta$, it is easy to check that $(\theta\chi\delta_h - \chi\delta_h + \Omega_M - \Delta\theta\delta_l - \theta\chi\delta_l) > 0$. Thus $\mathcal{L}(\Delta) > 0$ and then $\mathcal{D}'_{D,M}(\Delta) > 0$.

Case 1.2. When $\beta = \alpha+\gamma+\eta$, $\mathcal{L}(\Delta)$ is reduced to $8\alpha\eta^2\theta\Lambda\delta_l(\alpha+\gamma+\eta) > 0$. Then $\mathcal{D}'_{D,M}(\Delta) > 0$.

Thus, when $\beta \le \alpha+\gamma+\eta$, $\mathcal{D}'_{D,M}(\Delta) > 0$.

Case 2. When $\beta > \alpha+\gamma+\eta$, we have

$$\lim_{\Delta\to 0}\mathcal{L}(\Delta) = 2\alpha\eta\theta\Lambda\delta_l\mathcal{T}_1\mathcal{T}_3,$$

where

$$\mathcal{T}_1 = (\theta-1)\chi\delta_h + \mathcal{T}_2 - \theta\chi\delta_l,$$

$$\mathcal{T}_3 = \alpha-\beta+\gamma+\eta+\delta_h(\chi-\theta\chi) + \mathcal{T}_2 + \theta\chi\delta_l,$$

$$\mathcal{T}_2 = \sqrt{(\alpha-\beta+\gamma+\eta+\chi(1-\theta)\delta_h + \chi\theta\delta_l)^2 + 4\beta\eta}.$$

There are two cases.

Case 2.1. When $\mathcal{T}_1 \le 0$, $\mathcal{L}(\Delta) < 0$ for $\Delta \in [0, +\infty)$. Thus, $\mathcal{D}'_{D,M}(\Delta) < 0$.

Case 2.2. When $\mathcal{T}_1 > 0$, let $(\theta\chi\delta_h - \chi\delta_h + \Omega_M - \Delta\theta\delta_l - \theta\chi\delta_l) = 0$, we have a solution

$$\Delta^* = \frac{2\eta(\alpha+\beta+\gamma) + (\alpha-\beta+\gamma)^2 + \eta^2 - 2\chi(\alpha-\beta+\gamma+\eta)\left((\theta-1)\delta_h - \theta\delta_l\right)}{2\theta\delta_l(\beta-\alpha-\gamma-\eta)} > 0.$$

Note that when $\mathcal{T}_1 > 0$, we have $2\eta(\alpha+\beta+\gamma) + (\alpha-\beta+\gamma)^2 + \eta^2 - 2\chi(\alpha-\beta+\gamma+\eta)\left((\theta-1)\delta_h - \theta\delta_l\right) > 0$. This is because we need to ensure that

$$(\mathcal{T}_2)^2 - ((1-\theta)\chi\delta_h + \theta\chi\delta_l)^2 > 0 \Rightarrow 2\eta(\alpha+\beta+\gamma) + (\alpha-\beta+\gamma)^2 + \eta^2 - 2\chi(\alpha-\beta+\gamma+\eta)\left((\theta-1)\delta_h - \theta\delta_l\right) > 0.$$

Thus, $\mathcal{D}'_{D,M}(\Delta) > 0$ when $\Delta \in (0, \Delta^*]$ and $\mathcal{D}'_{D,M}(\Delta) < 0$ when $\Delta > \Delta^*$.

Q.E.D.

References

Chen, R., Peter, B., Joshua, S., 2003. An evaluation of alternative forecasting methods to recreation visitation. *Journal of Leisure Research*, 35(4), 441-454.

Keyes, K., C. Rutherford, A. Hamilton, J. Barocas, K. Gelberg, P. Mueller, D. Feaster, N. El-Bassel, M. Cerda. 2022. What is the prevalence of and trend in opioid use disorder in the United States from 2010 to 2019? Using multiplier approaches to estimate prevalence for an unknown population size. *Drug and Alcohol Dependence Reports*, 3 100052.